Mutational Analysis of the dsRNA Binding Domain of Vaccinia Virus E3 Protein

by

Kevin James Dick

A Thesis submitted to the Faculty of Graduate Studies of

The University of Manitoba

in partial fulfilment of the requirements of the degree of

MASTER OF SCIENCE

Department of Medical Microbiology

University of Manitoba

Winnipeg

Copyright © 2011 by Kevin James Dick

Abstract

Vaccinia virus E3 protein is known to bind double-stranded RNA and mediate interferon resistance. Alanine scanning mutagenesis was performed on its dsRNA binding domain, sufficient for wild-type tropism and immune suppression *in vitro*, and dsRNA binding and host range function assayed. Residues involved in dsRNA binding were required for host range function; however, seven dsRNA binding mutants were unable to rescue ΔE3L replication. Utilizing recombinant viruses, non-rescue mutants were unable to inhibit protein Kinase R phosphorylation despite dsRNA binding. Furthermore, host range was found to correlate with cytokine suppression and replication in IFN stimulated Huh7R cells. Additionally, no direct association was found between dsRNA binding and PKR interaction, refining the suppression model. Novel protein-protein interactions were discovered between E3 and cellular proteins via differential gel electrophoresis. This study represents the first full mapping of E3 residues involved in dsRNA binding and tropism, forming a basis for future study.

Acknowledgements

First, I would like thank my supervisor, Dr. Jingxin Cao for his guidance. I would also like to thank my committee members, Dr. Shawn Babiuk and Dr. Xiao-Jian Yao for their suggestions and support in completion of my thesis. I would also like to acknowledge lab members Yvon Deschambault, Peter Chen and Jocelyn Lee for their assistance.

I would also like to express my gratitude to the Natural Sciences and Engineering Research Council of Canada and the Manitoba Health Research Council for providing financial support during my studies. Additionally, I would like to thank the National Microbiology Laboratory of the Public Health Agency of Canada for support of this research and use of its facilities.

Finally, my family and friends for their encouragement, and my wife for her love and patience.

“The key purpose of education is not to validate ignorance, but to overcome it.”

- Lawrence M. Krauss

Table of Contents

List of Figures

List of Tables

List of Abbreviations

APC	Antigen Presenting Cell
ASC	Apoptosis-associated Speck-like protein containing a CARD
B/R	Poly I:C binding with rescue phenotype
B/NR	Poly I:C binding with non-rescue phenotype
CARD	Caspase Recruitment Domain
Cbr1	Carbonyl Reductase 1
CEV	Cell-associated Enveloped Virion
CMV	Cytomegalovirus
COP	Copenhagen Strain
COP-REV	Copenhagen ΔE3L Revertant virus
ΔE3L	E3L deletion mutant
DIGE	Differential Gel Electrophoresis
DRBD	Double-stranded RNA Binding Domain
DRBP	Double-stranded RNA Binding Proteins
EEF1A1	Eukaryotic Elongation Factor 1-α-1
EEF1G	Translation Elongation Factor 1 gamma
EEV	Extracellular Enveloped Virion
eIF2a	Eukaryotic Translation Initiation Factor 2α
EMCV	Encephalomyocarditis virus
GPT	Xanthine-guanine phosphoribosyltransferase
IEV	Intracellular Enveloped Virion
IFN	Interferon
IL	Interleukin
IMV	Intracellular Mature Virion
IPS-1	Interferon Beta Promoter Stimulator 1
IRF	Interferon Regulator Factor
ISG	Interferon Stimulated Gene
LANCL1	LanC-like protein 1
LPS	Lipopolysaccharide
LRR	Leucine Rich Repeats
MCMV	Mouse Cytomegalovirus
MDA5	Melanoma Differentiation Associated gene 5
MHC	Major Histocompatibility Complex
MPA	Mycophenolic Acid
MS	Mass Spectroscopy
MVA	Modified Vaccinia Ankara strain
NB/NR	Non-poly I:C binding with non-rescue phenotype
NFkB	Nuclear Factor kB
Nk	Natural Killer cells

NLR	NOD-Like Receptor
OAS	2'-5'-Oligoadenylate Synthetase
PACT	PKR Activator
PAMP	Pathogen Associated Molecular Pattern
pIC	Polyinosinic:polycytidylic acid
PKR	Protein Kinase R
PPI	Protein-protein Interaction
PRR	Pattern Recognition Receptor
PS	Phosphotidylserine
RIG-I	Retinoic Acid Inducible Gene 1
RLR	RIG-I like Receptor
RNAi	RNA Interference
RSV	Respiratory Syncytial virus
TBK1	TANK Binding Kinase 1
TBP	TATA Binding Protein
TLR	Toll-Like Receptor
TNF-a	Tumor Necrosis Factor alpha
VITF	Viral Intermediate Transcription Factor
VSV	Vesicular Stomatitis virus
WR	Western Reserve strain
ZBD	Z-DNA Binding Domain

1.0 Introduction

1.1 General Features of Poxviruses

Poxviridae are a diverse family of large double-stranded (ds) DNA viruses which replicate exclusively in the cytoplasm of host cells (Moss, 2007). They exhibit a varied host range; some members are specific to a single host, such as the Variola virus, the causative agent of Smallpox, while others, such as Vaccinia virus display a broad host range (Damon, 2007). Poxviruses encode a number of proteins which counter host viral defense mechanisms; this is in part due to the large protein coding potential of their genomes, ranging from 130-300 kb (Werden et al., 2008).

Poxviruses are divided into the subfamilies *Chordopoxvirinae*, which infect vertebrates and *Entomopoxvirinae*, which infect insect hosts (McFadden, 2005). *Chordopoxvirinae* include 8 genera: *Orthopoxvirus, Parapoxvirus, Avipoxvirus, Capripoxvirus, Leporipoxvirus, Suipoxvirus, Molluscipoxvirus*, and *Yatapoxvirus*. Of the *Chordopoxvirinae, Orthopoxviruses* have been the most thoroughly studied. This genera includes Cowpox, Ectromelia virus, Monkeypox, Variola and Vaccinia species, which display ~200 kb genomes and a varied host range (Moss, 2007). *Orthopoxviruses* encode a number of host range genes (Section 1.3), though none is fully conserved (Werden et al., 2008). Vaccinia virus is the prototypical *Orthopoxvirus* for laboratory study having been used as a vaccine against Variola.

The first Poxvirus genome completely sequenced was Vaccinia virus strain Copenhagen (COP), followed by Variola isolates allowing comparison of conserved elements (Goebel et al., 1990)(Shchelkunov et al., 1993; 1996). Poxviruses possess a linear genome bookended with inverted terminal repeats and conserved elements located centrally (Gubser et al., 2004). A total of 21 Poxvirus genomes were compared to define a minimal Poxvirus genome, containing 49 orthologs, displaying ~90% homology (Upton et al., 2003).

Poxviruses replicate exclusively in the cytoplasm of host cells, thus requiring their own replicative machinery. The virions are packaged with early transcription factors as well as RNA polymerase to initiate viral gene expression on infection (Moss, 2007). Poxviruses express their own mRNA capping enzymes and RNA polymerase (Broyles, 2003), DNA polymerase (Challberg and Englund, 1979; Earl et al., 1986) and factors to replicate in quiescent cells (Lin et al., 1992; Moss, 2007).

As poxviruses are important human and animal pathogens, an improved understanding of their pathogenesis is needed to prevent and treat infections as well as develop new vaccines. Although the current vaccine used for Smallpox is known to produce long lasting antibody (B cell) and cellular (T effector and central memory) immunity (Puissant and Combadière, 2006), due to the scarification technique and live virus used, significant risks are present especially for immunocompromised individuals (Liu et al., 2010).

Smallpox is no longer the scourge of humanity it once was, due to the Pan-American Health Organization and later the World Health Organization's efforts to eradicate the disease through global vaccination campaigns. However, Poxvirus infection in livestock and zoonotic infections are still prevalent. Poxvirus infections of domesticated animals especially sheep, goats and cattle are a source of significant financial burden in affected areas. Conversely, zoonotic outbreaks of Monkeypox have been documented in Congo (Rimoin et al., 2010), as well as outbreaks in the mid-western United States (Control, 2003). Human infections with Yatapox and Cowpox viruses have also been documented, with the immunocompromised at greatest risk (Essbauer et al., 2010). Recently an outbreak of human Buffalopox infections occurred in India, reinforcing the association of zoonotic infections with animal husbandry (Damie et al., 2011). Vaccinia infections have also been documented in Brazil (Nagasse-Sugahara et al., 2004)(Damaso et al., 2000), and in the United States (Hughes et al., 2011); these cases have been potentially linked to Smallpox vaccination efforts (Moussatché et al., 2008). Cases from laboratory exposures have also arisen, leading to recommendation of Smallpox vaccination for those working with unattenuated Vaccinia strains (MacNeil et al., 2009). Bioterrorism risks are also present due to retained Smallpox stocks throughout the globe, and the ability to bioengineer Smallpox based on available Variola genome sequences (Henderson et al., 1999)(McFadden, 2010). These risks have lead to the development of

Orthopoxvirus inhibiting compounds and renewed interest in improving the Smallpox vaccine (Smee, 2008)(Kennedy et al., 2009).

1.1.1 Poxvirus Structure and Replication

Mature virions possess a dumbbell shaped core in addition to a core membrane studded with spikes (Moss, 2006; Pogo and Dales, 1969). Poxvirus virions are divided into 4 subtypes: intracellular mature virions (IMV), intracellular enveloped virions (IEV), cell associated enveloped virions (CEV) and extracellular enveloped virions (EEV). Of these 4 types, IMVs are the most abundant (Smith and Law, 2004), however, the ratios vary between viral strains (Payne, 1980). IMVs possess a single membrane thought to be formed *de novo* or a double membrane acquired from Golgi transit (Condit et al., 2006). Membrane wrapped IMVs are IEVs and can bud through the plasma membrane but remain associated with the cell surface forming CEVs. Once on the cell surface, CEVs can polymerize actin allowing cell-to-cell spread or detach becoming EEVs (Smith et al., 2002). The outer envelope of EEVs can easily be disrupted, making investigation of their properties difficult (Roberts and Smith, 2008). IMVs are only released from lysed cells, and are thought to be the main vehicle of dissemination to other hosts (Ichihashi and Oie, 1996), while EEVs are thought to be important for spread of Poxviruses within a host (Blasco and Moss, 1991; Payne, 1980).

1.1.2 Attachment and Entry

Poxvirus IMVs and EEVs enter host cells via different mechanisms, fusing with the cellular membrane or entering by endocytosis, respectively (Ichihashi and Oie, 1996; Vanderplasschen et al., 1998). Currently, no single cellular receptor for Poxvirus entry has been discovered, indicating potential entrance by a more generalized mechanism. EEV entry has been studied by immunofluorescence, supporting endocytic entry and pH dependent release of the viral core following endosome fusion with the outer membrane (Vanderplasschen et al., 1998). IMVs do not display pH dependence, but their entry is impaired by depletion of membrane cholesterol indicating potential lipid-raft involvement (Carter, 2005). Based on analysis of knockout mutant viruses, 8 viral proteins have been found to be necessary for entry of IMVs: A16L, A21L, A28L, G3L, G9R, H2R, J5L and L5R (Moss, 2006; Senkevich et al., 2005).

Recently, apoptotic mimicry has been supported as the mechanism of entry for IMV, with cells displaying blebing in response to exposed phosphytidylserine (PS) on IMVs (Mercer and Helenius, 2008). This macropinocytotic feature is actin-dependent, and involves uptake of extracellular fluids and molecules into vacuoles up to 10 μm in diameter. This response can be induced by necrotic cells, apoptotic bodies, bacteria or viruses and causes cell-wide membrane ruffling or blebing (Sieczkarski and Whittaker, 2005). Investigation of Vaccinia PS based entry has shown the involvement of cellular Epidermal Growth Factor Receptor,

p21, Protein Kinase C and serine and threonine kinases (Mercer and Helenius, 2008). Further study has supported macropinocytosis as a general IMV entrance mechanism, though strain specific differences in host factor involvement between Vaccinia Western Reserve (WR) and International Health Department-J strains have been shown (Mercer and Helenius, 2010).

Study of Poxvirus spread indicates that spread outpaces replication kinetics. It was discovered that early in infection A33R and A36R are expressed, leading to a 'marked' phenotype and resistance to superinfection, greatly increasing infection efficiency (Doceul et al., 2010).

1.1.3 Early, Intermediate and Late Gene Expression

Poxvirus gene expression takes place in 3 phases; early, intermediate and late, with each stage producing transcription factors for the subsequent stage. However, at least 1 round of DNA replication is required prior to intermediate gene expression (Broyles, 2003; Moss, 2007). Following entry, the viral core is transported via microtubules adjacent to the nucleus and transcription is initiated (Smith et al., 2003). Early transcription is driven by the transcription factors D6R and A7L (Broyles and Fesler, 1990; Gershon and Moss, 1990), which interact with the early promoter leading to early gene transcription, which peaks ~1.5 hrs post infection (hpi) (Broyles, 2003; Davison and Moss, 1989). The 9 subunit viral RNA polymerase transcribes viral genes and bears similarity to eukaryotic and

prokaryotic RNA polymerases (Davis et al., 2002; Murakami et al., 2002; Patel and Pickup, 1989). In the early phase of viral expression a number of immune suppression factors are produced including E3L, K3L and B18R (Moss, 2007). Cell activation and growth are also stimulated leading to the 'lumpy skin' associated with Poxvirus infection through secretion of viral growth factor, showing Epidermal Growth Factor homology (da Fonseca et al., 1999; Twardzik et al., 1985).

Six intermediate genes have been identified: A1L, A2L G8R, I8R, K2L and I3L. A1L, A2L and G8R have been found to function as late gene transcription factors (Zhang et al., 1992). Intermediate gene expression requires 3 viral intermediate transcription factors (VITF) denoted VITF 1-3. VITF-1 composed of the RPO 30 subunit of the viral RNA polymerase, VITF-2 being host encoded, consisting of a complex of p137 and G3BP (Katsafanas and Moss, 2004), and VITF-3 formed by a complex of A8R and A23R (Broyles, 2003). Intermediate transcription also produces variable length transcripts based on analysis of the viral J3 elongation factor (Xiang et al., 2000).

Late transcription involves production of components necessary for virion assembly and initiation of infection. The 3 late transcription factors have been found to be non-redundant, all being required for late transcription (Moss, 2007). Late transcription also appears to utilize host TATA binding protein (TBP). TBP knockdown reduces late transcription and TBP has the capacity to interact with late promoters (Knutson et al., 2006). Assembly follows late protein translation, leading

to the 4 virion types released by budding, actin-polymerized spread or cell lysis (Section 1.1.1).

1.1.4 Genome Replication

Genome replication takes place adjacent the rough endoplasmic reticulum of infected cells (Schramm and Locker, 2005; Tolonen et al., 2001). Vaccinia encodes its own DNA polymerase (E9L), nucleoside triphosphatase (D5R) and DNA ligase (A50R) for genome replication (Challberg and Englund, 1979; Earl et al., 1986) (Evans et al., 1995; Evans and Traktman, 1987) (Moss, 2007). Following replication, concatamers of the viral genome are separated by H6R, K4L and A22R, and are packaged following late gene translation of virion components (Moss, 2007). Manipulation of Poxvirus genomes is possible via plasmids bearing flanking regions of genes, allowing both deletions and insertions through homologous recombination.

1.2 Interactions between Poxviruses and Innate Immunity

The innate immune response involves chemical and physical barriers, immune cells including antigen presenting cells (APC) as well as cellular detectors and signaling molecules. Through co-evolution between hosts and pathogens a number of features have developed in each. Hosts detect pathogen associated molecular patterns (PAMPs), these are conserved viral, bacterial or fungal

components, or products of infection, recognized as non-host by membrane bound or cytoplasmic pattern recognition receptors (PRRs). The major PRR groups being Toll-like receptors (TLRs), nuclear oligomerization domain (NOD)-like receptors (NLRs) and Retinoic Acid Inducible Gene 1 (RIG-I) like receptors (RLRs) (Biron and Sen, 2007). Outside of these families, fungal specific C-type lectins have been discovered and plants encode resistance proteins to detect pathogens (Lee and Kim, 2007). In the case of viral infection, detection of PAMPs by host PRRs lead to innate immune activation including IFN production, stimulation of pro-inflammatory cytokines, upregulation of antiviral genes transcription and induction of the anti-viral state (Biron and Sen, 2007). Pathogens have also developed means to subvert these detectors, their signaling and their downstream effectors. The pattern recognition hypothesis was first put forward by Janeway in 1989, and has been strongly supported in the decades of innate immune research that followed (Janeway, 1989). As the subject of this thesis is viral infection and more specifically dsRNA, innate immune components relevant to these subjects will be highlighted.

Innate immune responses shape the acquired immune response, leading to humoral and/or cellular immune responses such as the B and T cell based immunity evoked by smallpox vaccination (Henderson et al., 1999; Liu et al., 2010). Innate immune activation triggers inflammation and recruitment of immune cells to sites of infection through cytokines and chemokines, respectively (Biron and Sen, 2007). It also polarizes the acquired immune response through induction

of co-stimulatory molecules on APCs and secretion of cytokines (Biron and Sen, 2007).

1.2.1 Pattern Associated Molecular Patterns

PAMPs are conserved structural components or products of pathogen replication detected by PRRs. In the case of bacteria these are often cell wall components such as peptidoglycan, lipopolysaccharide, toxins or CpG DNA (Meylan et al., 2006). Similarly, fungal PAMPs are generally cell wall components, encompassing mannoproteins, β-glucans and zymosan. Alternatively, viral PAMPs are mainly nucleic acids, both genomic or produced during infection, including ssRNA, 5′ triphosphate RNA and dsRNA (Biron and Sen, 2007). In the context of Poxvirus infection dsRNA is produced in the cytoplasm during convergent transcription of viral genes (Jacobs and Langland, 1996; Jacquemont and Roizman, 1975), the overlaps forming dsRNA and being detected by cytoplasmic RLRs and IFN inducible genes Protein Kinase R (PKR) and 2'-5'- Oligoadenylate Synthetase (OAS) (Biron and Sen, 2007). RLR activation leads to IFN-β and Nuclear factor kB (NFkB) induction through IRF3/NFkB activation (Lee and Kim, 2007), while PKR and OAS halt protein synthesis. PKR and OAS are activated in a dsRNA dependent manner, halting protein synthesis via phosphorylation of Eukaryotic Translation Initiation Factor 2α (eIF2a) (Langland and Jacobs, 1992) and activation of RNase L to degrade cellular and viral RNA (Jacobs and Langland, 1996). RNA isolated from Vaccinia infection has been shown to activate dsRNA pathways, early and late

RNA having differential downstream effects (Myskiw et al., 2011). The Vaccinia E3 protein (Section 1.4) binds dsRNA and is thought to function through sequestering this PAMP to blunt innate immune activation, including detection by RLR and activation of PKR and OAS (Jacobs and Langland, 1996)(Barral et al., 2009). As dsRNA is a common viral PAMP, a number of viruses encode dsRNA binding proteins (DRBPs) (Section 1.4.2).

Thus, PAMPs alert the host to pathogen presence, being detected by a variety of receptors. Concerning these PRRs, TLRs have been implicated in the detection of viral, bacterial and fungal PAMPS, while NLRs appear to have bacterial specificity and RLRs viral specialization (Creagh and O'Neill, 2006).

1.2.2 Pattern Recognition Receptors

PRRs are cellular detectors of PAMPs that have co-evolved through host-pathogen interactions. They are located in the cytoplasm, endosomes and on the cell surface to detect both intra- and intercellular pathogens. The 3 major groups discovered are TLRs, NLRs and RLRs.

TLRs are transmembrane proteins containing 2 domains, a leucine rich repeat (LRR) domain that detects PAMPs and a TIR domain which signals through either MyD88 or TRIF/TRAM. TLRs are oriented with their TIR domains located on the cytoplasmic face of either the plasma membrane on endosomal membrane. TLRs interact with viral, fungal and bacterial components and were initially

discovered through fungal susceptibility of *Drosophila melanogaster* bearing mutations to the Toll/spatzle receptor (Lemaitre et al., 1996). Subsequently, a human homolog of Toll was discovered and TLR4 specificity for the lipid A component of bacterial lipopolysaccharide (LPS) determined (Medzhitov et al., 1997; Poltorak et al., 1998). A number of human TLRs have been discovered, with TLR1/2/6, TLR4 and TLR5 located on the cell surface and detecting bacterial lipoproteins, LPS and flagellin, respectively (Lee and Kim, 2007). Those important to the detection of viral infection are located endosomally and include TLR3, which detects dsRNA, and TLR7/8 that detect ssRNA. Also located endosomally, TLR9 is involved in detection of CpG DNA from bacterial infection (Creagh and O'Neill, 2006). Although Poxviruses replicate in the cytoplasm of infected cells, and thus would not activate endosomal detectors, infection can stimulate autophagy, enclosing viral components in endosomes and allowing TLR interaction (Delgado et al., 2009). TLR 1/2/6, 4 and 7/9 signal through MyD88 activating NFkB via IRAK and TRAF6 dependent pathways. TLR3 and TLR4 signal through TRIF, leading to TRAF6 or RIP1 based NFkB translocation and TANK-binding Kinase 1 (TBK1) associated IFN-β induction via interferon regulator factor (IRF) 3. Activation of NFkB leads to the expression of pro-inflammatory cytokines such as Tumor Necrosis Factor (TNF) -α, Interleukin (IL)-6 and IL-12 (Meylan et al., 2006).

NLRs are located in the cytoplasm and are activated by bacterial flagellin and peptidoglycan fragments as well as RNA and 'danger' signals. These proteins contain 3 domains: a LRR for detecting PAMPs, a NACHT domain and an effector

domain: Caspase Recruitment Domain (CARD), pyrin domain or a BIR domain (Meylan et al., 2006). NLRs have been implicated in the induction of pro-inflammatory cytokines through RIP2 based NFkB activation as well as interferon-β promoter stimulator 1 (IPS-1/MAVS/Cardif/VISA) dependent IRF3 induction of IFN-β. In the context of viral infection NOD2 has been found to activate IRF3 in response to ssRNA from Respiratory Syncytial (RSV), Vesicular Stomatitis (VSV) or Influenza virus infection (Lecat et al., 2010). NLRs are also involved in inflammasome formation, though their involvement in Poxvirus infection is unclear at present.

RIG-I, Melanoma Differentiation Associated gene 5 (MDA5) and LGP2 make up the RLR family, a group of soluble proteins involved in detection of nucleic acids. RIG-I detects viral RNA species in the cytoplasm, but was originally described in promyelocytic leukemia cells as a factor induced by retinoic acid treatment (Barral et al., 2009). RIG-I interacts with dsRNA signaling through IPS-1, leading to IRF3/7 based IFN-β induction and nuclear translocation of NFkB. Structurally, RIG-I contains a helicase domain, recognition domain with dsRNA/5' triphosphate specificity and a pair of CARD domains. The CARD domains have been found to interact with IPS-1, associated with the mitochondrial outer membrane, for downstream signaling (Kawai et al., 2005; Yoneyama et al., 2004)(Poeck and Ruland, 2011). RLR signaling through IPS-1 has also been found to be shaped by adaptor proteins, NEMO leading to NFkB and IRF3/7 activation, while FADD association initiates apoptosis via Caspase 8 (Yu and Levine, 2011).

Following the discovery of RIG-I, MDA5 and LGP2 were identified forming the RLR family (Yoneyama et al., 2005). LGP2, which lacks a CARD is thought to function as a negative regulator of this PRR pathway. RIG-I has been shown to decrease VSV and Encephalomyocarditis virus (EMCV) infection titers through RNA interference (RNAi) studies (Yoneyama et al., 2004), and RLRs importance has also been shown in TLR3 (dsRNA) deletion mouse models, which retained wild-type like response to VSV, LCMV and Mouse Cytolomegavirus (MCMV) infection (Meylan and Tschopp, 2006).

RIG-I and MDA5 both signal through IPS-1 leading to TBK1 and IRF3/7 dependent upregulation of IFN-β and TRAF mediated NFkB activation (Meylan et al., 2006; Lee and Kim, 2007). This signaling is opposed by viral DRBPs (Section 1.4.2) including Vaccinia E3 protein (Section 1.4), thought to sequester dsRNA, masking the PAMP from host detection. In response to 5′ triphosphate RNA, RIG-I has been shown to recruit apoptosis-associated speck-like protein containing a CARD (ASC) which activates Caspase 1, and displays IPS-1 signaling through CARD9/Bcl10 adaptors for NFkB activation (Poeck and Ruland, 2011). RIG-I has been found to have specificity for both positive and negative sense ssRNA viruses (Meylan and Tschopp, 2006). Additionally, RIG-I has been found to bind 5′ triphosphate RNA (Hornung et al., 2006) and polyinosinic:polycytidylic acid (pIC)/U:A synthetic RNA. The ligand(s) of MDA5 have been elusive, though specificity for picornaviruses (EMCV),long strands of dsRNA and pIC has been demonstrated (Yoneyama et al., 2005). RLRs have also been found to lack

specificity for host factors such as tRNA, 5′ capped and 3′ poly-A host mRNA, avoiding potential autoimmune activation (Barral et al., 2009; Onomoto et al., 2007). RLRs with non-functional CARD domains have been shown to inhibit RLR function, supporting LGP2's role as a negative regulator (Onomoto et al., 2007). CARD based signaling appears dependent on 4 cysteine residues with potential for coordination of zinc (Barral et al., 2009).

NFkB activation can be induced by TLRs and RLRs leading to the transcription of anti-viral genes, including pro-IL-1 and pro-IL-18 (Moss, 2007). Activation requires Caspase 1, which can be activated by NLR dependent inflammasome assembly (IPAF, AIM2 and NALP3) or RIG-I based ASC recruitment (Poeck and Ruland, 2011). Mature IL-1 and IL-18 increase leukocyte entry to infected areas, Nature Killer (Nk) cell activation and Th_1 polarization of the immune response (Lamkanfi and Dixit, 2009)(Creagh and O'Neill, 2006). Synergy is thus present between PRR pathways.

Vaccinia virus proteins have been found to inhibit a number of PRR pathway components, suppressing host response to PAMPs. Adaptor proteins MyD88, TRIF and TRAM, crucial in TLR signaling, are sequestered by A46R, while downstream IRAK-2 and TRAF6, involved in NFkB activation, are inhibited by A52R (Unterholzner and Bowie, 2008). IFN-β induction is suppressed by binding of TBK-1 by N1L and K7R proteins, inhibiting IRF3 activation by TLR and RLR signaling (Perdiguero and Esteban, 2009). Multiple proteins oppose the activation of NFkB, involved in pro-inflammatory cytokine induction, N1L binding the

inhibitor of IKK, while B14R and K1L inhibit the degradation of IkB and IkB-α, respectively (Perdiguero and Esteban, 2009; Unterholzner and Bowie, 2008). Poxviruses also oppose the secreted cytokines and effectors of these pathways.

1.2.3 Modulation of Cytokines by Poxviruses

Interferons and other cytokines are cell-signaling molecules that act in paracrine and autocrine fashions, recruiting immune cells and inducing the 'anti-viral state'. During infection, these are induced by the activation of NFkB, activator protein 1 and IRF family members initiated by PRRs (Biron and Sen, 2007). This transcription is actively suppressed during Poxvirus infection through inhibition and sequestering of proteins involved in PRR pathway signal transduction (Section 1.2.2).

IFNs have long been recognized for their anti-viral properties (Lengyel, 1987) and induction by viral PAMPs such as dsRNA (Sen and Lengyel, 1992). Pro-inflammatory cytokines include TNF-α, IL-1β, IL-6, IL-12, IL-18 and IFN-β. IFN-α, IFN-β and IFN-ω are designated Type I IFN. IFN-α and IFN-β share a common heterodimeric receptor which signals classically through the JAK/STAT pathway, leading to STAT1/2 phosphorylation and dimerization. Dimerized STAT1/2 recruit IRF9 forming the ISGF3 transcription factor which translocates to the nucleus leading to expression of interferon stimulated genes (ISGs) (Perdiguero and Esteban, 2009). The Type I IFN receptor also leads to the activation of Rac1 initiated by

VAV or GEF, which activates p38 through MAPK signaling. Activation of p38 regulates STAT based ISG transcription though activation of downstream kinases (Platanias, 2005). The phosphorylation of STAT1 is opposed by Vaccinia H1L/vH1, a virion component possessing phosphatase activity, suppressing initial IFN receptor signaling (Perdiguero and Esteban, 2009). Multiple innate pathways lead to Type I IFN expression, initial IFN-β expression requiring IRF3 activation, while subsequent IFN-α/β expression can be driven by IRF3, IRF5 or IRF7 (Taniguchi and Takaoka, 2001). ISGs include OAS (Section 1.2.4), PKR (Section 1.2.5) and ISG56 which halt translation, as well as ISG15 which has been found to modify proteins in a ubiquitin-like manner (Liu et al., 2011).

During induction of the anti-viral state, secreted IFN-β targets all nucleated cells and leads to the upregulation of major histocompatibility complex I, to present intracellular antigens, ISGs and activation of IFN-γ secretion by Nk cells. Intracellularly, IFN-β signaling induces IRF7 expression, capable of dimerization and induction of further IFN production, thus priming cells for IFN secretion in a positive feedback loop. ISGs induced by IFN include PKR, OAS, MxA and ADAR, which impart cellular resistance to infection (Biron and Sen, 2007). Other pro-inflammatory cytokines such as IL-6 target B cells/liver cells causing acute phase reactions, while IL-18 stimulate Nk and T cell IFN-γ production. At infection sites, TNF-α and IL-1 increase vascular permeability for leukocyte infiltration, the former activating monocytes and Nk cells and recruiting dendritic cells (DC) to infection

sites (Biron and Sen, 2007). IFNs thus alert both immune and systemic cells to the presence of infection.

Poxviruses secrete a number of cytokine receptor decoys that bind and inhibit the activities of host cytokines. IFN-α and β are opposed by B18R produced early in infection, while IFN-γ is suppressed by B8R (Alcami et al., 2000; Colamonici et al., 1995). TNF-α signaling is suppressed by K3R and the secreted receptor homolog A53R (HAGA and Bowie, 2005; Werden et al., 2008). Additionally, B15R and C12L oppose the pro-inflammatory IL-1β and 18, respectively (McFadden and Murphy, 2000). Thus, in addition to suppressing of IFN signaling, the activities of secreted cytokines are inhibited during infection.

1.2.4 2'-5'- Oligoadenylate Synthetase/RNase L

OAS is a cytoplasmic protein induced by type I IFN. OAS activation is dsRNA dependent, leading to the production of 2′5′ linked oligomers of ATP. These oligomers in turn activate latent RNase L degrading host and viral RNAs, thus abolishing translation (Castelli et al., 1998; Rebouillat and Hovanessian, 1999). Viral dsRNA genomes, type 1 IFN and pIC stimulation have been found to induce OAS expression (Lengyel, 1987). Vaccinia virus replication has been found to be uninhibited even in high cellular concentrations of OAS, demonstrating Vaccinia resistance to OAS in HeLa, L929 and CUI cells (Rice et al., 1984). Vaccinia is believed to suppress OAS through sequestering of dsRNA, required for OAS

activation. Supporting this, E3 has been found to suppress OAS activation during infection and inhibit transiently expressed OAS dependent RNase L activation in ΔE3L infected cells (Jacobs and Langland, 1996; Rivas et al., 1998). Four OAS family members have been identified: OAS 1-3 which differ in their number of subunits, and OASL an OAS-like protein (Melchjorsen et al., 2009; Rebouillat and Hovanessian, 1999). Though related, OAS1 induction has been shown to be IFN dependent, while OASL requires IRF3 activation (Melchjorsen et al., 2009).

Vaccinia virus recombinants have been constructed expressing OAS1, and found to inhibit its replication, but not that of VSV co-infection under IFN stimulation, showing potential OAS1 *Orthopoxvirus* specificity (Díaz-Guerra et al., 1997). This platform was also used to profile genes upregulated by OAS during infection, with ISGs, growth arrest and apoptotic factors displaying increased transcription (Domingo-Gil et al., 2010). OAS overexpression has been shown to inhibit cell growth, increase apoptotic sensitivity (Zhou et al., 1998) and contribute to the transcription of several ISGs (ISG15, IL-8, P54 and P56) (Malathi et al., 2005).

RNase L, when activated functions as a dimer, each monomer containing 9 ankyrin repeats. RNase L displays endoribonuclease activity, cleaving host and viral RNA. The cleavage of ssRNA by RNase L can generate short dsRNAs which activate cellular RLRs interlinking these innate immune pathways (Chakrabarti et al., 2011). Vaccinia C7L protein has been implicated in inhibiting the pro-apoptotic activity of RNase L (Perdiguero and Esteban, 2009).

1.2.5 Protein Kinase R

PKR is a cytoplasmic IFN inducible gene, which is capable of dimerization. PKR activation classically leads to the phosphorylation of the ribosomal subunit eIF2a at Ser51, inhibiting translation initiation (Garcia et al., 2006). Although the major function of PKR is thought to be inhibition of translation, PKR has been shown to be involved in NFkB activation, FADD based apoptosis initiation, and JNK/p38 signaling (Kirkegaard et al., 2004). It possesses a N-terminal dsRNA binding domain and C-terminal kinase domain, requiring dimerization and phosphorylation at Thr446 for activation (Robertson and Mathews, 1996). Interaction of PKR with dsRNA appears to be structural rather than sequence specific (Cohen-Chalamish et al., 2009; Heinicke et al., 2009), requiring a minimum of 16 bp to bind (Bevilacqua and Cech, 1996) and 33 bp to activate (Manche et al., 1992; Zheng and Bevilacqua, 2004). PKR has been shown to activate in the presence of dsRNA (Gilfoy and Mason, 2007; Meusel et al., 2002). PKR is preferentially activated by the presence dsRNA free of bulges or kinks (Cole, 2007; Lemaire et al., 2005). Based on decreased PKR activation to dsRNA possessing larger bulges, kinks and trans bulges, a model of PKR dimerization to a single face of dsRNA has been proposed (Heinicke et al., 2011). Alternatively, PKR can be activated by cellular PKR activator protein (PACT) due to cellular stress rather than dsRNA (Singh et al., 2011).

PKR was originally discovered through investigation of the mechanism of eIF2a phosphorylation inhibition by VAI RNA from Adenovirus (Schneider et al., 1985) (O'Malley et al., 1986), and its auto-phosphorylation following binding of dsRNA (Katze et al., 1987). Activation of NFkB by PKR induces the transcription of pro-inflammatory cytokines. Additionally, MKK6 based p38 activation by PKR leads to IFN and cytokine induction (Silva et al., 2004). Other roles of PKR include its requirement for TLR4 based apoptosis of macrophages and negative regulation of IFN-γ expression (Cohen-Chalamish et al., 2009; Hsu et al., 2004).

Vaccinia virus encodes 2 factors that oppose PKR pathways, K3L and E3L. K3 is a pseudo-substrate of PKR, displaying eIF2a homology, thus blunting the translation suppressive effects of PKR (Moss, 2007). Alternatively, E3 binds to dsRNA, required for PKR activation as well as interacts with PKR through both its domains (Romano et al., 1998; Jagus and Gray, 1994). Through mutational analysis of E3 (Section 1.4.1), 3 key amino acids involved in PKR-E3 interaction have been mapped and associations between PKR activation and E3 dsRNA binding have been demonstrated. Mutational analysis of PKR indicate that E3 can bind to both N and C-terminal regions of PKR, the former interaction being enhanced in the presence of dsRNA (Sharp et al., 1998). The major role of E3 is thought to be the inhibition of PKR activation, which will be explored in Section 1.4.1.

1.3 Poxvirus Host Range Genes

Poxviruses encode a number of genes that combat the host response including secreted proteins to bind host factors, inhibitors of apoptosis and suppressors of immune activation. A number of these factors, deemed host range genes, have been found to restrict viral replication in cell culture or *in vivo* when altered. These included Vaccinia: SPI-1, K1L, C7L, p28/N1R, B5R, K3L and E3L. K1L is an ankryin-repeat containing protein, required for replication in RK13 cells. K1L inhibits IkB-a degradation, thus suppressing NFkB activation. As well, K1L has been found to inhibit IFN stimulated effectors (Meng et al., 2009). C7L deletion in addition to K1L leads to restriction in PK1, RK13 and multiple human cell lines, while C7L deletion alone suppresses apoptosis and limits replication in hamster Dede cells (McFadden, 2005) (Werden et al., 2008). Serine Protease Inhibitor 1 (SPI-1) alteration has been has been found to restrict replication in PK15 and A549 cells, in addition to attenuating Vaccinia in a mouse model. P28/N1R, an E3-RING-finger ubiquitin ligase, involved in protein degradation and apoptosis suppression is required for mouse macrophage replication, while B5R, a membrane glycoprotein, activates Src allowing growth in VERO, CEF, PK15 and quail (QT-6) cells (Werden et al., 2008). The host range genes E3L and K3L appear to have functional synergy. E3 binding dsRNA required for PKR activation while K3, an eIF2a homolog, functioning as a pseudo-substrate for PKR (Werden et al., 2008). Deletion of K3L limits replication in BHK21 and mouse L929 cells, while E3L

deletion leads to reduced tropism, inhibiting growth in Vero, HeLa, CEF, IFN pre-treated Huh7R cells and murine DCs (Werden et al., 2008)(Arsenio et al., 2008). The innate immune suppressive features of E3 and current understanding its mechanisms of action will be covered in the following sections.

1.4 E3 Protein

E3 is a conserved Poxvirus protein expressed early in infection and known to suppress multiple innate immune pathways. E3 is a 25 kDa protein, also known as P25, possesses the ability to bind dsRNA (Chang et al., 1992). A second minor transcript is also produced through use of an alternate start codon, resulting in a 19 kDa product (Yuwen et al., 1993). The full-length protein contains 2 domains, a N-terminal Z-DNA binding (ZBD) domain and a C-terminal dsRNA binding domain (DRBD) (Moss, 2007). E3 is thought to function mainly by sequestering of dsRNA, masking it from host detection imparting IFN resistance and suppressing PKR and OAS activation (Beattie et al., 1995; Jacobs and Langland, 1996). Binding of dsRNA in order to suppress the immune response is a strategy employed by multiple viruses (Section 1.4.2).

The DRBD of E3 has been found to be sufficient for suppression of PKR, OAS and IFN resistance *in vitro*, while the ZBD is required for full pathogenesis *in vivo*. This difference in pathogenesis was explored via scarification, intracranial and intranasal infection models of C57BL/6 mice (Brandt et al., 2005; Brandt and

Jacobs, 2001; Kim et al., 2003). The ZBD's 3D structure has been determined and Z-DNA binding confirmed. The ZBD bears similarity to Zα family members, while the DRBD has not been crystalized due to aggregation (Ha et al., 2004; Kahmann et al., 2004). Resistance to apoptotic stress and transactivation of host genes including IL-6, NFAT and p53, using a transient reporter system, appear to be ZBD dependent (Kwon and Rich, 2005). Some role in the opposition of PKR activation has been observed for the ZBD, based on mutational analysis in *Escherichia coli*, specifically involving Trp66 (Romano et al., 1998). As the subject of this thesis regards the DRBD of Vaccinia E3, further discussion will focus on studies involving the full-length protein and/or its DRBD.

E3 displays cytoplasmic localization, though nuclear presence has been noted (Yuwen et al., 1993). The full-length protein shows dimerization potential and displays oligomerization at low salt concentrations, the DRBD remaining a dimer (Ho and Shuman, 1996a). Yeast two-hybrid studies utilizing Vaccinia WR have demonstrated protein-protein interactions (PPI) with human DHX9, MAST1, MAST2, MAST4, STAU 1 and STAU2, though interaction with PKR was absent (Van Vliet et al., 2009). Interaction with PKR involving both domains of E3 has been found, leading to the proposal of E3 suppressing PKR activation by interfering with PKR dimerization, or sequestering of dsRNA (Romano et al., 1998). PKR suppression is seen as a major role of E3, with studies showing its loss allowing replication of Vaccinia E3L deletion (vvΔE3L) mutants in HeLa cells (Langland and Jacobs, 2004). This was demonstrated by RNAi based PKR knockdown in HeLa

cells, showing recovery of host range and suppression of apoptosis in vvΔE3L infections (Zhang et al., 2008). E3 also antagonizes largely PKR-independent induction of IL-6 and IFN-β, associated with early and late viral RNA PAMPs, respectively (Myskiw et al., 2009). E3 also appears to play roles in cellular immunity. Infected DCs show increased pro-inflammatory cytokine secretion, T cell activation and sensitivity to TNF-α and IL-6 induction in ΔE3L but not wild-type Vaccinia infections (Deng et al., 2006). Supporting a potential role of E3 in systemic alteration of the immune responses, transgenic mice expressing E3 were found to be susceptible to *Leismania major* infection, displaying reduced antigen specific T-cell response (Domingo-Gil et al., 2008). During HeLa infection with Vaccinia Modified Vaccinia Ankara (MVA) strain ΔE3L, replication was halted at intermediate gene translation, though intermediate transcription remained unaltered, indicating a role in translation maintenance (Ludwig et al., 2006). Similar to the requirement of the ZBD of E3 for *in vivo* pathogenesis, PKR knockout wasn't sufficient to support vvΔE3L pathogenesis, even in triply deficient (OAS^- /PKR^-/MxA^-) c57BL/6 mice (Xiang et al., 2002). Recent studies utilizing vvΔE3L have supported E3's involvement in opposing ISG15 function (Guerra et al., 2008), IFN-λ responses (Bandi et al., 2010) and suppression of cytoplasmic stress granules following infection (Simpson-Holley et al., 2011).

Analyzing the DRBD, it appears sufficient to support many functions of E3 *in vitro*. In HeLa cells, the DRBD has been shown to blunt IFN-β responses to 5′ triphosphate RNA and dsDNA, likely functioning through suppression of RIG-I

pathways (Marq et al., 2009). The DRBD has also been shown to be sufficient to support replication in HeLa cells (Beattie et al., 1996). Later studies have identified the DRBD as sufficient to suppress dsDNA mediated IFN-β induction (Valentine and Smith, 2010), despite the DRBD's low affinity for DNA and DNA-RNA hybrids (Ho and Shuman, 1996a). Full length E3 and its DRBD have similar profiles of altered host gene expression, downregulating pro-inflammatory cytokine expression, antigen presentation and acute phase genes, this suppression being absent in vvΔE3L infections (Langland et al., 2006). Thus, in cell culture the DRBD is thought to function comparably to wild-type E3.

1.4.1 Mutational Analysis of E3

Mutational analysis of E3 has involved deletion/replacement studies (Section 1.4), truncation and individual amino acid (aa) mutations. Preliminary mutation of E3 involved Δ83 aa N-terminal truncation (E3L-C111) and C-terminal Δ7 and Δ26 aa truncations (E3L-Δ175), only the latter of which abolished dsRNA binding. The Δ7 and Δ26 mutants displayed impaired PKR suppression, while mutation of G164, K167 and A174 reduced dsRNA binding, correlating with impaired PKR inhibitory capacity (Chang and Jacobs, 1993). *In vivo*, E3L-Δ175 mutants have impaired intranasal pathogenesis in c57BL/6 mice, requiring ≥100 fold greater PFU infection than wild-type virus to cause mortality (Brandt and Jacobs, 2001). Based on conservation between 2 DRBDs (*E. coli* RNase III and *D. melanogaster* staufen), 14

aa's within E3's DRBD were mutated to alanine, 6 displaying impaired dsRNA binding: G124A, P135A, P148A, R167A, K168A and R171A (Ho and Shuman, 1996b). Based on a similar design strategy, residues W66, K167 and R168 were found to be important for E3's interaction and suppression of PKR (Romano et al., 1998).

1.4.2 dsRNA Binding Proteins

E3 is a member of a larger family of viral DRBPs, involved in the viral pathogenesis and suppression of host responses. These proteins are thought to oppose PRR detection of dsRNA and activation of dsRNA dependent ISGs. Other members include Reovirus S4 (Beattie et al., 1995), Influenza NS1 (Talon et al., 2000), Cytomegalovirus (CMV) pIRS1/pTRS1 (Marshall and Geballe, 2009), Ebola virus VP35 (Basler and Amarasinghe, 2009), Rotavirus NSP3, Epstein-Barr Virus SM and Herpes Simplex Virus 1 US11 proteins (George et al., 2009). NS1 has been shown to suppress IRF3 phosphorylation and downstream IFN induction (Talon et al., 2000), and in the case of defective NS1, increased IFN-β production was noted during infection (Donelan et al., 2003), potentially may be related to RIG-I activation. An IFN sensitive phenotype has been shown in Ebola virus bearing dsRNA-binding defective VP35 mutations (Basler and Amarasinghe, 2009). NS1 and VP35 expressed during infection have been shown to bind pIC beads, supporting its use in this study (Hale et al., 2010; Prins et al., 2010). CMV DRBPs

have also been used to rescue vvΔE3L replication and found to suppress PKR activation (Marshall and Geballe, 2009). Hence, E3 and its DRBP properties represent a common viral strategy to avert innate immune activation.

1.5 Rationale and Approach

The involvement of Vaccinia virus E3 protein in the suppression of PKR, OAS and RIG-I activation as well as resistance to the anti-viral effects of IFN has been shown. These features are thought to be largely due to the sequestering of dsRNA, a viral PAMP, binding via E3's C-terminal DRBD. *In vitro,* the DRBD has been found to be sufficient for many of E3's features; however, no direct experimental data are available to confirm the model that E3 functions through sequestering dsRNA (Section 1.4). Currently, only a few amino acids have been defined in relation to the dsRNA binding phenotype of E3, designed based on conserved residues between *E. coli* RNase III and *D. melanogaster* staufen DRBDs (Section 1.4.1). Many Poxvirus genomes have been sequenced allowing comparison of E3L orthologous sequences (Upton et al., 2003). In this study alanine scanning mutagenesis will be performed on all residues of the DRBD. We hypothesize that the conserved residues among E3L orthologs are of greater likelihood to be involved in the biological function of E3, and expected to differ from those determined by comparison with *E. coli* and *D. melanogaster* DRBDs (Section 1.4.1). Retention of dsRNA binding through use of pIC bead pulldown,

and rescue of ΔE3L virus replication in restrictive HeLa cell lines will be performed. These assays will form the first complete mapping of the DRBD of E3. This mapping will allow the correlation between dsRNA binding and host range function to be determined for exploration in this project and future studies.

A larger role than simple dsRNA binding is likely, due to the multiple pathways suppressed by E3 as well as the positive feedback of IFN induction (Section 1.2.3). This feedback loop induces further dsRNA interacting proteins (PKR, OAS, MxA), making competitive inhibition unlikely. DRBD dependent interaction with PKR in Yeast has been observed, and over-expression of the kinase defective PKR has also been shown to antagonize full-length E3 activity (Romano et al., 1998). Furthermore, deletion of the host range gene K1L (Section 1.3) increases PKR activation in response to early and late viral dsRNA, despite the presence of E3, indicating its role may lie outside sequestering of this PAMP (Willis et al., 2011). In concert with the implications of IFN induction these results support a role beyond dsRNA binding for E3.

After establishing the relationship between pIC binding and ΔE3L virus replication, recombinant Vaccinia viruses expressing individual mutations will be generated. These mutants designed to explore associations between binding, rescue, and alterations in E3's established properties (Section 1.4), such as differences in IFN resistance, cytokine induction and innate immune activation. As these features depend on different pathways, the role dsRNA binding plays in the function of E3 may be elucidated.

Previous interaction studies have also utilized full-length E3. Here for the first time we are aware, the PPIs of E3, N-terminal (E3L-C111) and C-terminal (E3L-Δ175) E3L truncations will be analyzed. These will be explored in HeLa cells via 2D Differential Gel Electrophoresis (DIGE) and identified through MALDI TOF/TOF mass spectrometry. Interaction with endogenously expressed PKR in both Huh7R and HeLa cells will be explored. GST tagged E3 mutants will be used to investigate the correlation of inhibition with PKR binding and test the current models of PKR-E3 interaction (Heinicke et al., 2011; Romano et al., 1998).

Through these experiments the role of dsRNA binding in innate immune suppression will be elucidated, along clarification of the role of E3 in alteration of cellular responses. Furthermore, this study will map key residues involved in dsRNA binding and support of viral replication, establishing a basis for future study.

2.0 Materials & Methods

2.1 Cell Culture, Media and Reagents

Cell Culture

HeLa, Huh7R and BHK21 cells were maintained in Dulbecco's modified Eagle's medium, supplemented with 10% fetal bovine serum and 1% penicillin-streptomycin-glutamine (Gibco Life Technologies), and incubated at 37°C in 5% CO_2.

Antibodies and Reagents

Total PKR antibodies were purchased from Cell Signaling Technologies. Phosphospecific PKR (Thr446) was acquired from Epitomics. Total eIF2a and phosphorylated-eIF2a were obtained from Biosource. β-Actin antibody was purchased from Sigma (Clone AC-15, A5441). Polyclonal E3L antibodies 1 and 2 were produced in rabbits against peptide 161-174 (KADGKSKRDAKNNA) and 88-101 (VSREKSMREDHKSF) by GenScript. Polyclonal antibodies against vvD12L (RERDAIKSNNHLTE) and vvG8R (TPGNTDAFSREYSM) were produced in rabbits (GenScript USA Inc.). Rabbit Glutathione S-Transferase (GST) antibody was purchased from Sigma (G7781). Purified E3 protein was made by GenScript. PBS pH 7.4 [137mM NaCl, 2.68 mM KCl, 10.1 mM Na_2HPO_4 anhydrous, 1.76mM KH_2PO_4] used throughout pulldowns. Sodium dodecyl sulfate (SDS) sample buffer

used throughout Western blotting made at 6x concentration [10% SDS, 30% glycerol, 0.5 M Tris/SDS pH 6.8, 6 mg Bromophenol Blue, 0.8 M β-mercaptoethanol] and diluted with ddH_2O.

Primers

Primers used throughout experiments synthesized by NML Genomics Core except E3L-C111n, synthesized by Eurofins MWG Operon. Primer sequences (Table 1).

Primer Name	Sequence (5′->3′)
NcoE3L-F1	ATGTCTAAGATCTATATTG
NcoE3L-R1	**TCA**GAATCTAATGATGACG
coE3Ln80NHA	TAGGATCCATGTACCCCTATGACGTGCCCG ATTACGCCATGAGCAAGATCTACATCG
E3Lc175cSMA	TAACCCGGGTCACCCGTCGGCCTTGTCGAACACGCGC
E3L-C111n	AAGGATCCATGTACCCCTATGACGTGCCCGATTACGCCATG
E3LcSMA	CCCGGG**TCA**GAATCTAATGATGACGTAACC
pDEST-rev	GATACTGCAGCGTACGT
GSTnBAM	GATCGGATCCATGTCCCCTATACTAGGTTATTG
GSTnSMA	AATTGGGCCCAGTTGCGCCTTGGTCTAG
GST-TGA-SMA	GATCCCCGGG**TCA**ACGCGGAACCAGATCCGATTTTGG
PJS5-FR1	GTTATTGCTCAGCGGTGGC
GPT-C	ATTAGCGACCGGAGATTGGCGGGA
GAPDH N	TTACTCCTTGGAGGCCATGT
GAPDH C	AAGGTGAAGGTCGGAGTCAACGGA
vvA1 N	ATGGCTAAGCGAGTAAGCCTTCCAGAT
vvA1 C	TTACAATAAACTCCGTAGAGAAATATC
vvD12 F	ACCTCAGCGCACGCAATAAACTGTTCA
vvD12 R	AGTCATACTAGAATAAAGCAGCGAGT
vvG8 F	AATGTAGACTCGACGGATGAGTTA
vvG8 R	TCGTCATTATCCATTACGATTCTAGTT

Table 1 – Sequences of PCR Primers with stop codon bolded and restriction enzyme cut sites underlined.

2.2 Western Blotting

SDS-PAGE

Western blots were performed using Criterion XT 4-12% Bis-Tris gels with MOPS XT Running buffer (Bio-Rad Laboratories Inc.). All samples were prepared in 1xSDS buffer, with Benchmark pre-stained protein ladder and MagicMark XP Western Protein Standard ladders (Invitrogen Life Technologies).

Transfer of Western Blots

Criterion XT gels (Bio-Rad Laboratories Inc.) were transferred to Amersham Hybond-C Extra nitrocellulose membranes (GE Healthcare Life Sciences) via semi-dry electrophoretic transfer (Tyler Research Corporation). Transfers were performed for 1 hr at 150mA per full Criterion gel. Hybond-c extra membrane was pre-soaked in transfer buffer at room temperature and shaken at 30 RPM for 10 mins prior to use. Blocking, primary and secondary antibody incubations performed in 5% skim milk TBS 0.2% Tween (TBST) with shaking at 80-100 RPM. Washes performed with TBST.

Developing

Western Blots were developed with Immobilon Western Chemiluminescent HRP Substrate (Millipore) or Western Lighting ECL (PerkinElmer Inc.). Immobilon

reagents were mixed and equilibrated to room temperature for 10 mins prior to use. Kodak X-Omat Blue film used to capture chemiluminescence.

2.3 Design, Synthesis and Cloning of E3 Mutants

Design of E3 mutants

Alanine scanning mutagenesis was performed on all residues in the dsRNA binding domain of Vaccinia virus Copenhagen E3. In the case of an alanine, valine substitution was performed. All mutants were synthesized in pUC57 with BamHI (N-terminal) and SmaI (C-terminal) restriction enzyme cut sites (GenScript USA Inc.). An alignment was performed between E3L orthologs from 5 *Chordopoxvirinae* members: Vaccinia virus Copenhagen, Myxoma virus , Capripox virus, Yaba Monkey Tumor Virus and Swinepox virus (Appendix 1). This alignment allowed differentiation of highly conserved (Table 2) and lowly conserved residues (Table 3) in the dsRNA binding domain.

F101A	N123A	A150V	A175V
D103A	E124A	V152A	K176A
I105A	Y125A	I154A	D180A
P106A	C126A	G156A	L182A
K108A	Q127A	F159A	L182A/L183A
K109A	T129A	G164A	L183A
I110A	R131A	K167A	I187A
I111A	W133A	R168A	I187A/I188A
W113A	F135A	D169A	I188A
K114A	G141A	A170V	R189A
N117A	S143A	K171A	F190A
P118A	N144A	N172A	
I121A	P146A	N173A	
I122A	F148A	A174V	

Table 2 – Conserved residues among E3L orthologs and substitutions synthesized in pUC57. Residue mutations indicated.

M80A	S93A	T120A	R157A
A81V	M94A	I128A	V158A
D82A	R95A	K130A	D160A
V83A	E96A	D132A	K161A
I84I85A	D97A	S134A	A162V
I84A	H98A	R136A	D163A
I85A	K99A	I137A	K165A
D86D87A	S100A	E138A	S166A
D86A	D102A	S139A	L177A
D87A	V104A	V140A	A178V
V88A	A107A	P142A	V179A
S89A	D112A	S145A	K181A
R90A	D115A	C151A	G184A
E91A	A116V	D153A	Y185A
K92A	V119A	D155A	V186A

Table 3 – Low Conservation Residues among E3L orthologs and substitutions synthesized in pUC57. Residue mutations indicated.

Cloning of Synthesized E3L mutants

Synthesized E3L mutants in pUC57 were triple digested with restriction enzymes XmaI, high fidelity BamHI and ApaLI (NEB Ltd.) for 1 hr at 37°C. ApaLI digest was performed in order to cleave pUC57, reducing background. QIAquick PCR purification was performed following digestion (QIAGEN Inc.). The pJS5 plasmid containing EGFP as well as p7.5gpt was cut with XmaI and high fidelity BamHI (NEB Ltd.) for 1 hr at 37°C, and purified as above. Ligation was performed at 16°C overnight with T4 DNA Ligase (NEB Ltd.). JM109 cells were transformed with ligated vectors (Promega Corp.), and spread on LB agar plates containing 200 µg/mL carbenicillin. Colonies were PCR screened using goTaq® Green Master Mix (Promega Corp.), with NcoE3L-F1 and PJS5-FR1 primers. Positive clones were grown overnight at 37°C in *E. coli* Fast-Media Amp TB (InvivoGen) shook at 300 RPM. Plasmids were purified using QIAprep Miniprep Spin columns (QIAGEN Inc.). E3L mutants in pJS5 constructs were sequenced using NcoE3L-F1 primer, by NML Genomics Core, to confirm the mutation.

2.4 Construction of Recombinant Vaccinia Copenhagen Viruses

All recombinant viruses generated summarized in Table 5.

Alanine Mutant Recombinant Viruses

Mutants of interest (I110A, N123A, C126A, F135A, F159A) were cloned into pΔE3L vector previously described (Arsenio et al, 2008). pΔE3L plasmid itself and

pJS5 plasmids carrying each mutant were digested using NdeI and NheI (Fermentas – Thermo Fisher Scientific Inc.) for 1 hr at 37°C in order to transfer the cassette bearing EGFP and an E3L mutant between plasmids (Figure 1) . Following digestion agarose gel electrophoresis was performed (1% agarose, TBE, 120V) and QIAquick Gel Extraction protocol utilized to purify NdeI/NheI cut pΔE3L vector and inserts bearing the pJS5 multiple cloning site with the E3L mutant of interest and EGFP (QIAGEN Inc.). Ligation, transformation and plating as previously described. Positive pΔE3L colonies were confirmed by PCR screening, grown in TB Amp and plasmids purified as above.

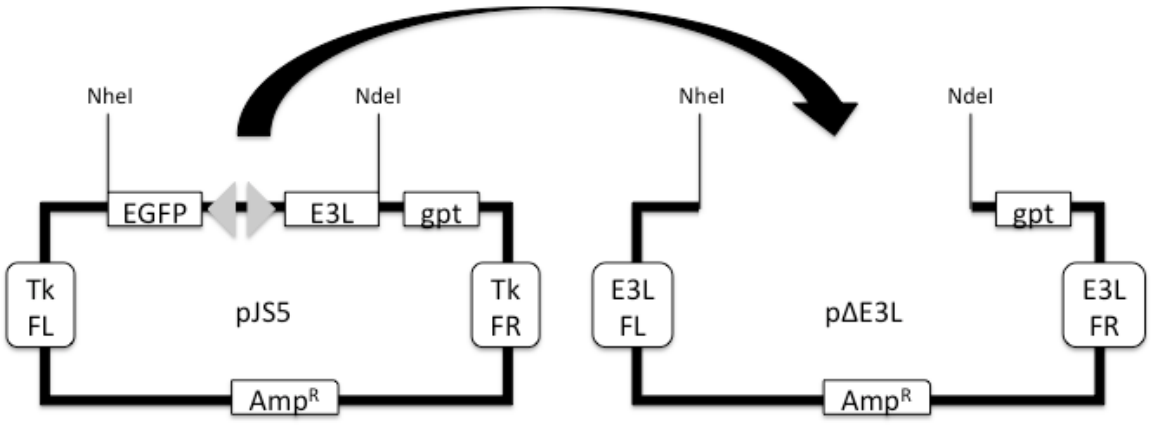

Figure 1 – Transfer of E3L/EGFP cassette from pJS5 to pΔE3L. NheI and NdeI cut sites indicated. TK FL/FR: Thymidine Kinase locus, flanking left and right. E3L FL/FR: E3L locus, flanking left and right.

GST Tagging of Mutant E3

N-terminal GST fusion proteins were constructed for recombinant virus generation and transient expression. GST fusions of codon optimized Vaccinia E3L, C-Terminal 25 amino acid truncation (E3L-Δ175) or 80 amino acid N-terminal truncation (E3L-C111) mutant and I110A, N123A, C126A, F135A and F159A mutants were cloned into Gateway® pENTR™3C Dual Selection vector (Invitrogen Life Technologies) (truncations described in Myskiw et al., 2009). Clonase II (Invitrogen - Life Technologies) recombination was performed between the pENTR™3C vectors and pDEST™27 to produce N-terminal GST fusion products. Colonies were screened using forward primers and pDEST-rev primers. GST alone was amplified from pDEST™27 via iProof PCR reaction (Bio-Rad Laboratories Inc.) using N-terminal GSTnBAM to add a BamHI restriction site and C-terminal GST-TGA-SMA to add a stop codon (TGA) and a SmaI site. BamHI/SmaI double digest (NEB Ltd.) was performed on the gel extracted GST for 1 hr at 37°C, followed by QIAquick PCR Purification (QIAGEN Inc.) and ligation into previously BamHI HF/XmaI cut pΔE3L as above. N-Terminal GST fusion mutants were iProof (Bio-Rad Laboratories Inc.) PCR amplified from pDEST™27 using GSTnSMA and E3Lc175cSMA or E3LcSMA, for E3L-Δ175 and all other mutants, respectively. PCR products digested with SmaI (NEB Ltd.) for 1 hr at 37°C then QIAquick PCR purified, gel extracted and ligated into pΔE3L as above. The pΔE3L constructs were transformed and plated as above. PCR screening was performed using the reverse primer GPT-C with forward primers of coE3Ln80NHA for E3L and E3L-Δ175, E3L-

C111n for E3L-C111, NcoE3L-F1 for alanine mutations and GSTnBam for GST alone. Positive colonies were grown and plasmids purified as above.

Transfection of Recombination Plasmids

Transfections were performed using Attractene Transfection Reagent (QIAGEN Inc.). Plasmids were diluted in RNase free water to a final volume of 20 µl for infections in 6-well plates, 40 µl for 100 mm dishes. Prior to transfection plasmids were sterilized for 15 mins at 85°C. Transfections were incubated in serum-free DMEM for 15-30 min at room temperature with Attractene reagent as per Qiagen protocol. Transfection reaction dripped onto monolayers covered by recommended volumes of media following incubation.

Recombinant Copenhagen Viruses

BHK21 cells in 6-well plates at 70-80% confluence were infected with Vaccinia Copenhagen wt virus at a MOI of 0.2. After 1 hr virus was aspirated and 2ml of media added to each well. Cells were then transfected with pΔE3L constructs in order to replace the wt E3L locus with a mutant E3L gene, EGFP expression construct for identification and p7.5gpt for selection. Plaques were observed via fluorescent microscopy. Plaque picking to purify virus was initiated following the fourth passage in selective media containing mycophenolic acid (MPA) as Xanthine-guanine phosphoribosyltransferase (GPT) was inserted into the E3L locus along with the mutant E3 protein to allow growth in MPA (Falkner &

Moss, 1988). For plaque picks, confluent BHK21 monolayers were infected with serial dilutions of recombinant virus for 1 hr at 37°C. Following infection the virus was aspirated and monolayer overlayed with Type VII Agarose and 2xMEM supplemented with FBS and antibiotics. Plaques were detected by fluorescent microscopy and picked 24-48 hpi. Plaques were picked through use of plugged sterilized Pasteur pipettes. Each plaque was picked and then placed in 1ml of DMEM supplemented with 2% FBS and antibiotics in cryotubes. Following collection, 3 rounds of freeze/thaw at -80°C were performed to release virus. Subsequent rounds of plaque picking performed using collected samples.

Determination of Copenhagen Recombinant Virus purity

In order to determine the purity of recombinant viruses produced from wt Copenhagen strain Vaccinia Virus, confluent BHK21 monolayers were infected with virus at an MOI of 1 and RNA collected at 24 hpi using RNeasy kits (QIAGEN Inc.). On column RNase-free DNase digest was performed and cDNA produced using QuantiTect Reverse Transcription kit (QIAGEN Inc.). RT-PCR was performed using forward primers terminating on the mutated nucleotides corresponding to the alanine substitution, giving them specificity to mutant or wild-type E3L cDNA. Both wild-type and mutant sequence primers were used to amplify cDNA from mutant virus infections. Amplifications were performed with an annealing temperature of 57.5°C using goTaq® Green Master Mix (Promega Corp.). Primers were HPLC purified prior to use (Table 4).

Primer Name	Sequence (5′->3′)
110-wt	GATGTTATTCCGGCTAAAAAAAT
110-mut	GATGTTATTCCGGCTAAAAAAGC
123-wt	GCTAACCCTGTCACCATTATTAA
123-mut	GCTAACCCTGTCACCATTATTGC
126-wt	CACCATTATTAATGAGTACTG
126-mut	CACCATTATTAATGAGTACGC
135-wt	CTAAGAGAGATTGGTCTTTT
135-mut	CTAAGAGAGATTGGTCTGCT
159-wt	GACATCGACGGAAGAGTATT
159-mut	GACATCGACGGAAGAGTAGC

Table 4 – RT-PCR primer sequences used to analyze purity of recombinant I110A, N123A, C126A, F135A and F159A viruses. Nucleotide differences in 3′ regions of primers underlined.

Recombinant COP-ΔE3L Viruses

BHK21 monolayers in 6-well plates at 70-80% confluence were infected with COP-ΔE3L virus at a MOI of 0.2. After 1 hr virus was removed and 2 ml of media added to each well. Monolayers were then transfected with pJS5 constructs in order to replace the thymidine kinase locus of the virus with EGFP and an E3L mutant. Recombinant COP-ΔE3L virus was used directly for rescue assays in HeLa cells as well as Poly IC pulldown experiments.

GST-E3L fusion Recombinant COP-ΔE3L Viruses

COP-ΔE3L virus was used to create recombinants of GST-E3L and GST-C111 E3L due to their ability to support replication in HeLa cells. Following infection and transfection as above, virus was collected at 24 hpi and used to infect 80% confluent HeLa monolayers. Virus was passaged in HeLa cells 4 times, the

first infection collected at 24 hpi and subsequent infections at 48 hpi. Plaque picking performed as previously described for GST-Δ175 and GST alone viruses, while plaque picking was performed in HeLa cells rather than BHK21 cells for GST-E3L and GST-C111 viruses due to replication competence in HeLa cells.

Virus	**Recombinant Basis**	**Locus of Insertion**
I110A	wt COP	E3L
N123A	wt COP	E3L
C126A	wt COP	E3L
F135A	wt COP	E3L
F159A	wt COP	E3L
GST-E3L	COP-ΔE3L	Thymidine Kinase
GST-Δ175	COP-ΔE3L	Thymidine Kinase
GST-C111	COP-ΔE3L	Thymidine Kinase
GST	COP-ΔE3L	Thymidine Kinase

Table 5 – Summary of recombinant Vaccinia viruses generated. Viral basis and location of gene insertion indicated.

Amplification of virus

Confluent BHK21 monolayers were infected with 300 µl of virus for 1 hr at 37°C followed by addition of DMEM media supplemented with 2% FBS and antibiotics. Virus was then collected at 24 hpi following 3 rounds of freezing and thawing at -80°C. Amplification was repeated as required. Titrations were performed as described below (Section 2.6).

2.5 Host Range Rescue in HeLa cells

Host Range Rescue in HeLa cells

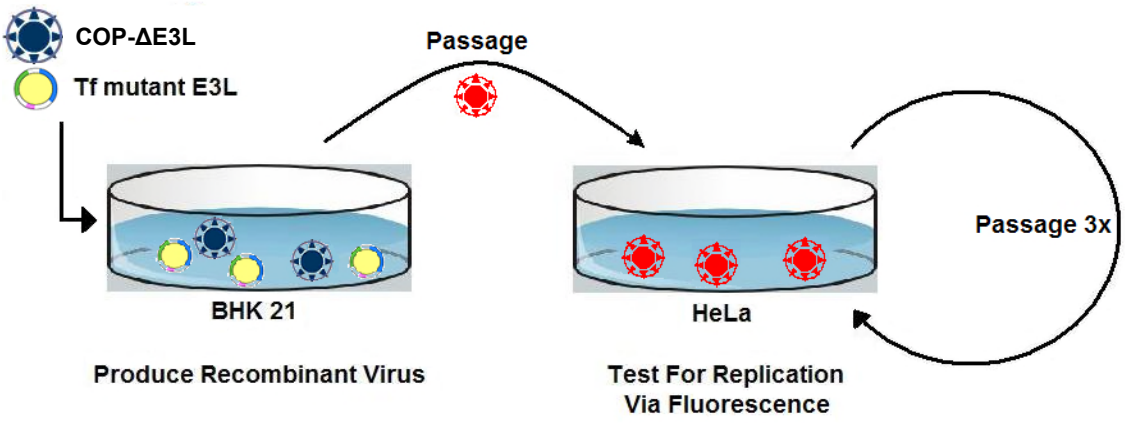

Figure 2 - Assay of ΔE3L rescue in HeLa cells. Tf: transfection, red virus indicates formation of recombinant virus.

Passaging of Mutant Vaccinia in Rescue Assays

Recombination was performed as described above. Infected BHK21 cells were collected at 24 hpi and freeze/thawed 3 times at -80°C to release recombinant virus. HeLa monolayers were infected at 70-80% confluence. Initial HeLa passages were collected at 24 hpi while subsequent passages were collected at 48 hpi. Three passages total were performed in HeLa cells (Figure 2). Initial passage in HeLa cells infected with 100 µl of virus while subsequent passages were infected with 200 µl of collected virus from previous passage. Plaque formation was determined by fluorescent microscopy.

2.6 Interferon Sensitivity Assays in Huh7R Cells

Interferon Sensitivity Assays

Huh7R monolayers of 80% confluence were pretreated overnight at 37°C with 0, 10, 100, or 1000 U/ml of IFN-β1 (PBL Biomedical Laboratories). Monolayers were infected with MOI 1 of COP-REV, COP-ΔE3L, I110A, N123A, C126A, F135A or F159A mutants for 1 hr at 37°C. Media was aspirated after 1 hr, monolayers washed with PBS, and replaced with media of the previous IFN-β1 concentrations. Viruses were grown at 37°C and collected 5 and 24 hpi.

Titration of Interferon Sensitivity Assays

Collected virus was used to infect confluent 12-well BHK21 plates. Serial dilutions of collected virus were used to infect the monolayers in triplicate. Infections were incubated for 1 hr at 37°C, media was replaced following aspiration. Plaques were counted using fluorescent microscopy at 24 hpi.

2.7 Pulldown

Pulldown protocol based on Abcam immunoprecipitation protocol (Abcam, 2011). Non-denaturing lysis buffer [20 mM Tris HCl pH 8, 137 mM NaCl, 10% Glycerol, 1% Triton-X, 2 mM EDTA].

Pre-Clear Beads

Glutathione beads provided in slurry (Thermo Fisher Scientific Inc.) were cleared and resuspended in non-denaturing lysis buffer. This was not required in the case of pIC beads due to their storage in non-denaturing lysis buffer. 300 µl of non-denaturing buffer was added to 200 µl of glutathione beads, vortexed and centrifuged at 5000g for 2 mins, and the supernatant discarded. This was repeated 3 times, with final resuspension in 350 µl of non-denaturing lysis buffer.

Cell Lysate Preparation

BHK21 or HeLa monolayers were infected and transfected at ≥70% confluency and harvested at times indicated. Cell collection was performed over ice, and collection tubes were pre-cooled on ice. Monolayers harvested 24 hrs after infection/transfection.

Media was then removed from the monolayer, and washed with ice cold PBS. 350 µl of ice cold PBS added to each well of a 6-well plate or 1 ml added to a 100 mm dish and cells collected using a 25 cm cell scrapers. 70 µl of collected

as a pre-pulldown sample remaining cells in PBS pelleted (5000g/4 min) and aspirated. Pre-pulldown samples stored at -20°C for up to 6 hrs. Pellets for pulldown were lysed in 1 ml of non-denaturing lysis buffer with protease inhibitor added per 100 mm dish or 350 µl per well of a 6-well plate (1 tablet Roche complete protease inhibitor cocktail/15 ml lysis buffer). Cells lysed on ice for 30 mins, with resuspension every 10 mins. Cellular debris was removed through centrifugation at 5400g/10 min in a 4°C pre-cooled centrifuge. Supernatant transferred to new 1.5 ml Eppendorf tube.

Pulldown

100 µl of beads in non-denaturing lysis buffer were added to each sample from a 100 mm dish, or 40 µl to samples collected from a 6-well plate. Samples were incubated at room temperature and rotated end-over-end for 2 hrs. Samples were then pelleted, the supernatant discarded and washed with 500 µl (100 mm dish) or 300 µl (6-well plate) non-denaturing lysis buffer, vortexed and centrifuged at 5400g for 2 mins. Washes were performed 3 times. Final resuspension was done in 350 µl 1x SDS (100 mm dish) or 200 µl 1x SDS (6-well plate) and incubated at 95°C for 10 mins, resuspended at 5 mins. Beads pelleted through centrifugation at 5000g for 2 mins. Supernatant retained for Western blot.

2.7.1 Glutathione Pulldown

Immobilized Glutathione was purchased from Pierce (cat# 15160). Glutathione beads were pre-cleared prior to use as described above.

2.7.2 Polyinosinic:Polycytidylic Pulldown

Poly IC bead preparation protocol was developed in house. Polyinosinic acid (pI, Sigma, cat # P4154), polycytidylic acid (pC, Sigma, cat # P4903) and polyinosinic: polycytidylic acid (pIC, Sigma, cat# P1530) were bound to CNBr-activated Sepharose 4B beads (GE Healthcare Life Sciences, cat# 17-0430-01). 10U/ml of RNase Inhibitor added to non-denaturing lysis buffer used in pulldowns performed with Poly IC beads (NEB Ltd., cat# M0307L). Lysate preparation and pulldown performed as described previously.

Bead Preparation

1 g of sepharose beads were washed 40 ml 1 mM HCl, mixed and centrifuged at 1000g for 5 min. Supernatant was removed; this process was repeated 5 times.

Conjugation of Beads

Beads of pI, pC or pIC were prepared in coupling buffer [0.1 M $NaHCO_3$ pH 8.3 containing 0.5 M NaCl] at 10 mg/ml. 20 mg of pIC in 4 ml total volume coupling buffer was added to bead preparation and rotated end-over-end for 2 hrs at room temperature. Unconjugated pIC was removed by washing 5 times in 5x volume of coupling buffer and centrifuged at 1000g for 5 mins, removing supernatant after each wash. Active sites of the Sepharose beads were blocked by incubation with 0.1 M Tris-HCl pH 8.0 for 2 hrs at room temperature.

Washing of beads

Alternating low pH and high pH buffers were used to wash the beads, 3 cycles of washes were performed. Low pH buffer: 0.1 M sodium acetate pH 4.0, 0.5 M NaCl; high pH buffer: 0.1 M Tris-HCl pH 8.0, 0.5 M NaCl. Following the final wash, beads were stored as 50% slurry in non-denaturing lysis buffer at 4°C until use.

2.7.3 dsRNA Pulldown

BHK21 monolayers were infected for Glutathione pulldown as previously described using GST tagged pJS5 E3L constructs. Non-denaturing lysis was performed as previously described, with 500 U/ml of RNase inhibitor added to the non-denaturing lysis buffer to preserve cellular RNA. Following washes of the

beads, pulled down RNA was extracted with a RNeasy kit (QIAGEN Inc.). DNase treatment followed elution, with TURBO™ DNase (Ambion Biosystems). Reverse-Transcription was performed using QuantiTect Reverse Transcription Kit (QIAGEN Inc.). RT-PCR was performed using GAPDH, vvA1, vvD12 and vvG8 primer sets on both cDNA and eluted RNA.

2.7.4 PKR-Pulldown

PKR-Pulldown in HeLa cells

Pulldown was performed as in glutathione pulldown protocol. Monolayers were pre-transfected with 1650 ng of DNA 2 hrs prior to infection with MOI 2 of COP-REV virus. Samples were collected 10 hpi and proteins harvested as previously described. Precipitation was performed with 175 µl of pre-cleared glutathione beads.

2.8 Real-Time Quantitative PCR

RNA Extraction and cDNA synthesis

RNA extractions were performed using RNeasy kits (QIAGEN Inc.). Monolayers were homogenized via QiaShredder columns (QIAGEN Inc.). Optional on-column RNase free DNase treatment was performed on samples for RT-PCR, and incubated for twice the recommended time. Samples for quantitative

real-time PCR were DNase treated following elution with TURBO™ DNase (Ambion Biosystems). RNA concentration and purity analysis performed via NanoDrop 2000 (Thermo Fisher Scientific Inc.). Reverse-Transcription was performed using QuantiTect Reverse Transcription Kit (QIAGEN Inc.).

Real-time Quantitative PCR

Real-time PCR was performed in 96-well PCR plates on a StepOnePlus Real-time PCR System (Applied Biosystems) using TaqMan Gene expression Master Mix (cat# 4369016) (Applied Biosystems). Triplicate 25 µl reactions were performed (5 µl cDNA (25ng), 0.42 µl 60x primer, 7.09 µl H_2O, 12.3 µl TaqMan Mix) and gene expression normalized against human β-Actin (AIWRF6D). Human IFN-β, IL-6 and TNF-α primers used in analysis (Applied Biosystems). Gene expression analyzed via StepOne software v2.0 via comparative CT method (Applied Biosystems).

2.9 Silver Staining

All solutions prepared in a total volume of 250 ml in ddH_2O: fixing solution (75 ml MeOH, 25 ml glacial Acetic Acid), sensitization solution [75 ml MeOH, 10 ml sodium thiosulphate (5%w/v), 17 g sodium Acetate], silver solution [25 ml silver nitrate solution (2.5% w/v)], developing solution [6.25 g sodium carbonate, 100 µl formaldehyde (37% w/v) added just prior to use], stopping solution [3.65 g EDTA-Na_2-H_2O].

Silver Staining of Glutathione Pulldown

Glutathione pulldown was performed as described in the previous section; lysate in 1xSDS buffer was used for silver staining. Silver staining was performed on Criterion XT 4-12% Bis-Tris gels (Bio-Rad Laboratories Inc.). Silver staining was performed using PlusOne™ Silver Staining Kits (GE Healthcare Life Sciences) using a modified protocol obtained from Dr. M. Carpenter at the National Microbiology Laboratory. Solutions were removed following each step.

All incubations were performed at room temperature on a shaking table in autoclave Pyrex dishes (80 RPM). Gels incubated overnight in fixing solution. Followed by an additional 15 min incubation in fresh fixing solution. Sensitization solution was added for thirty mins followed by three 5 min washes in ddH_2O. Silver solution added for twenty min followed by two 1 min washes in ddH_2O. Developing solution was added for 4 to 6 mins and stopping solution was added when ladder was still discernable and incubated for 10 min. 3 washes in ddH_2O were performed prior to imaging.

2.10 2D Difference Gel Electrophoresis and MS/MS Analysis

2D DIGE Protocol

Samples were prepared as previously described for Glutathione pulldown. Protein sample was harvested 8 hpi from HeLa monolayers infected with COP-REV at a MOI of 2. Monolayers were pre-transfection with pJS5 constructs at 1650

ng/100 mm dish 4 hrs prior to infection using Attractene reagent for GST-Δ175 and GST alone. Pulldown lysates were shipped to Applied Biomics (Hayward, CA, USA) on dry ice for pairwise 2 CyDye analysis (GST-E3L vs. GST-Δ175, GST-E3L vs. GST-C111, GST-E3L vs. GST). Samples were normalized for protein concentration and linked to CyDye followed by isoelectric focusing and SDS-Page.

Spot Identification

Spots for identification were determined based on differential expression and protein concentration as determined by imaging of DIGE gels. Spots were identified via MALDI-TOF/TOF analysis following in-gel trypsin digestion (Applied Biomics).

MS/MS Data Analysis

MS Data analysis was performed by Applied Biomics Inc., based on PMF and MS/MS data of picked spots. NCBinr database used as reference, with the addition of Vaccinia COP genome and GST tag sequences.

3.0 Results

3.1 Alanine Scanning Mutagenesis of the dsRNA Binding domain of E3 for pIC binding

In order to determine residues potentially involved in dsRNA binding alanine scanning mutagenesis was performed on all residues in the DRBD. Polyinosinic: polycytidylic acid coated beads were used to pulldown the mutant proteins. Three coating procedures for constructing the beads were evaluated the specificity of dsRNA binding of both virally expressed and *E. coli* expressed E3 protein (Figure 3). Both sequentially and directly coated beads, pI->C and pIC, respectively, were able to pulldown E3L; subsequent experiments were performed with pIC beads. While they did not bind to ssRNA pC beads, thus, the binding is specific to dsRNA. Both pre- and post-pulldown samples of each mutant expressed in an infection context were analyzed by Western blotting for the presence of E3. Each mutant was tested at least twice to confirm binding, representative example of pIC binding are presented in Figure 4, displaying consistent pre-pulldown E3 levels, while pulldown samples displayed a largely binary pattern. Of the 115 mutants evaluated (Appendix 2A, 2B)(Table 6), all were expressed and 18 were unable to bind pIC, all of these residues being highly conserved among E3L orthologs (Appendix 1). One low conservation mutant, E138A, displayed reduced binding indicating potential importance in dsRNA binding.

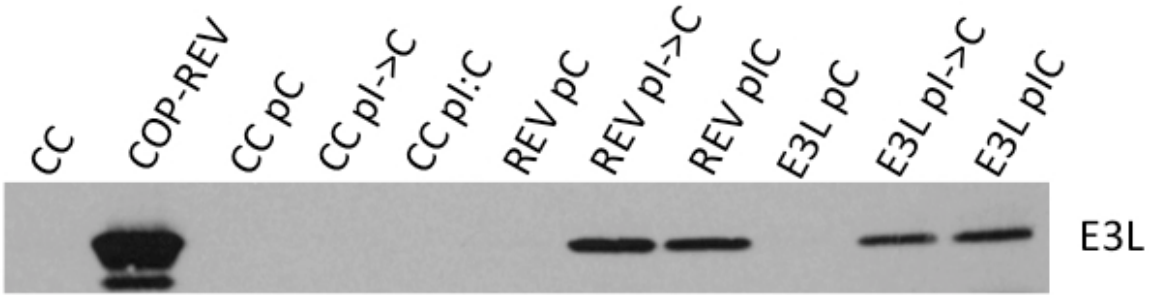

Figure 3 – Verification of dsRNA binding of E3. BHK21 cells were infected with COP-REV at an MOI of 0.1 and grown overnight. Both cell control and infected cells were precipitated with pC, pI->C and pIC coated sepharose beads. Purified E3L, 12.5 mg, added to non-denaturing lysis buffer containing bead types as control. Probed with vvE3L #2 antibody.

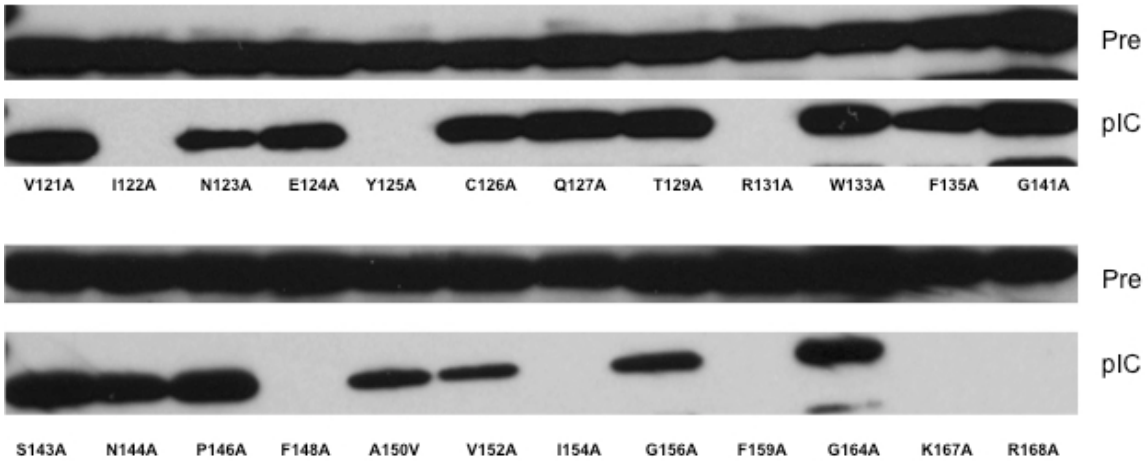

Figure 4 – Representative pIC pulldown of E3 mutants in BHK21 cells. Highly conserved (Table 2) and non-conserved (Table 3) residues analyzed. Pre- and post-pulldown samples shown. 1 µg of DNA transfected per well of a 6-well plate following 1 hr infection with MOI 0.2 COP-ΔE3L virus. Samples collected after growth overnight. Western blots probed with rabbit polyclonal vvE3L #2 antibodies.

3.2 Functional Analysis of Mutant E3 proteins, based on Rescue of ΔE3L Virus in HeLa cells

Mutant E3 proteins were assayed for their ability to rescue the replication of ΔE3L Vaccinia virus in HeLa cells. Recombinant viruses of each mutant based on ΔE3L expressing EGFP were produced in BHK21 cells, which are permissible to ΔE3L virus replication. Three passages in HeLa cells were performed and monolayers examined via fluorescent microscopy for viral plaque formation, which will indicate E3 mutant rescue of ΔE3L replication in HeLa cells. Representative rescue assay, Figure 5, displays overlays of cell monolayers and fluorescently detected plaques showing productive and non-productive replication. Of the 115 mutants, 25 were unable to rescue ΔE3L, while 2 displayed very limited growth (Table 6). All low conservation residues (Table 3) were supportive of replication including E138A.

All rescuing mutants display pIC binding, while a negative correlation between pIC binding and rescue in HeLa cells was observed in 7 mutants: N123A, E124A, Q127A, T129A, W133A, F135A, G156A (Table 7). These 7 mutants being unable to rescue ΔE3L replication in HeLa cells, although they bound pIC beads. Mapping of key E3 residues involved in pIC binding, support of ΔE3L replication and disconnections displayed in Figure 6.

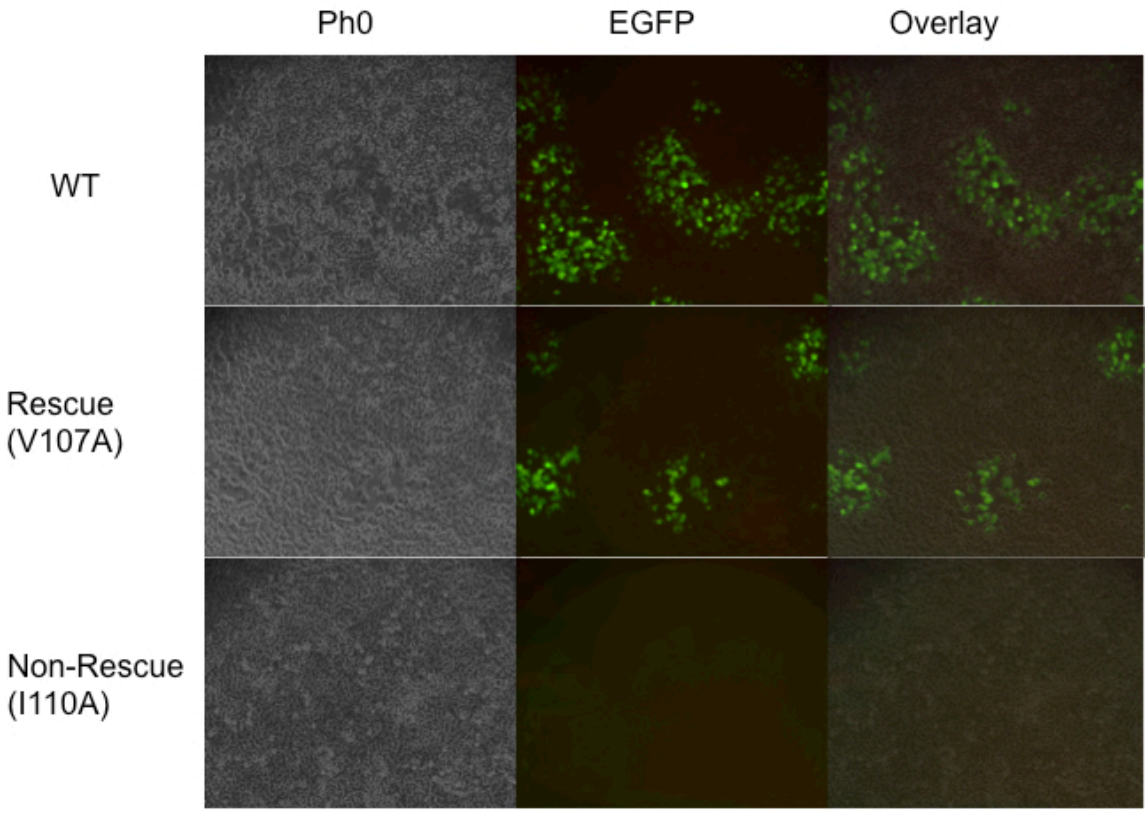

Figure 5 – HeLa rescue assay, representative of wild-type, rescue and non-rescue E3 mutants. Support of COP-ΔE3L replication was evaluated via fluorescent microcopy. Viral plaques were identified through EGFP expression, 3 passages in HeLa cells performed. Ph0 images converted to gray scale and EGFP images overlayed. Images collected 24 hpi.

Mutant	Rescue	pIC	Mutant	Rescue	pIC	Mutant	Rescue	pIC
WT	Rescue	Bound	A116V	Rescue	Bound	D155A	Rescue	Bound
M80A	Rescue	Bound	N117A	Rescue	Bound	G156A	N	Bound
A81V	Rescue	Bound	P118A	Rescue	Bound	R157A	Rescue	Bound
D82A	Rescue	Bound	V119A	Rescue	Bound	V158A	Rescue	Bound
V83A	Rescue	Bound	T120A	Rescue	Bound	F159A	N	N
I84/I85A	Rescue	Bound	I121A	Rescue	Bound	D160A	Rescue	Bound
I84A	Rescue	Bound	I122A	N	N	K161A	Rescue	Bound
I85A	Rescue	Bound	N123A	N	Bound	A162V	Rescue	Bound
D86/ D87A	Rescue	Bound	E124A	N	Bound	D163A	Rescue	Bound
D86A	Rescue	Bound	Y125A	N	N	G164A	Rescue	Bound
D87A	Rescue	Bound	C126A	Rescue	Bound	K165A	Rescue	Bound
V88A	Rescue	Bound	Q127A	N	Bound	S166A	Rescue	Bound
S89A	Rescue	Bound	I128A	Rescue	Bound	K167A	N	N
R90A	Rescue	Bound	T129A	N	Bound	R168A	N	N
E91A	Rescue	Bound	K130A	Rescue	Bound	D169A	Rescue	Bound
K92A	Rescue	Bound	R131A	N	N	A170V	Rescue	Bound
S93A	Rescue	Bound	D132A	Rescue	Bound	K171A	N	N
M94A	Rescue	Bound	W133A	N	Bound	N172A	Rescue	Bound
R95A	Rescue	Bound	S134A	Rescue	Bound	N173A	Rescue	Bound
E96A	Rescue	Bound	F135A	N	Bound	A174V	N	N
D97A	Rescue	Bound	R136A	Rescue	Bound	A175V	N	N
H98A	Rescue	Bound	I137A	Rescue	Bound	K176A	Rescue	Bound
K99A	Rescue	Bound	E138A	Rescue	Bound	L177A	Rescue	Bound
S100A	Rescue	Bound	S139A	Rescue	Bound	A178V	Rescue	Bound
F101A	Rescue	Bound	V140A	Rescue	Bound	V179A	Rescue	Bound
D102A	Rescue	Bound	G141A	Rescue	Bound	D180A	Rescue	Bound
D103A	Limited	Bound	P142A	Rescue	Bound	K181A	Rescue	Bound
V104A	Rescue	Bound	S143A	Rescue	Bound	L182A	Limited	Bound
I105A	N	N	N144A	Rescue	Bound	L182/ L183A	N	N
P106A	Rescue	Bound	S145A	Rescue	Bound	L183A	N	N
A107A	Rescue	Bound	P146A	Rescue	Bound	G184A	Rescue	Bound
K108A	Rescue	Bound	T147A	Rescue	Bound	Y185A	Rescue	Bound
K109A	N	N	F148A	N	N	V186A	Rescue	Bound
I110A	N	N	Y149A	Rescue	Bound	I187A	Rescue	Bound
I111A	Rescue	Bound	A150V	Rescue	Bound	I187/ I188A	N	N
D112A	Rescue	Bound	C151A	Rescue	Bound	I188A	Rescue	Bound
W113A	N	N	V152A	Rescue	Bound	R189A	Rescue	Bound
K114A	Rescue	Bound	D153A	Rescue	Bound	F190A	Rescue	Bound
D115A	Rescue	Bound	I154A	N	N			

Table 6 – Summary of E3 mutant rescue of Vaccinia ΔE3L in HeLa cells. Results representative of 3 passages in HeLa cells. pIC binding phenotype of each mutant indicated, highly conserved residues: grey; lowly conserved: white (Appendix 1).

Mutant	Rescue	pIC Binding
N123A	N	Bound
E124A	N	Bound
Q127A	N	Bound
T129A	N	Bound
W133A	N	Bound
F135A	N	Bound
G156A	N	Bound

Table 7 – Negative correlations between pIC binding of mutant E3 proteins and support of ΔE3L viral replication in HeLa cells.

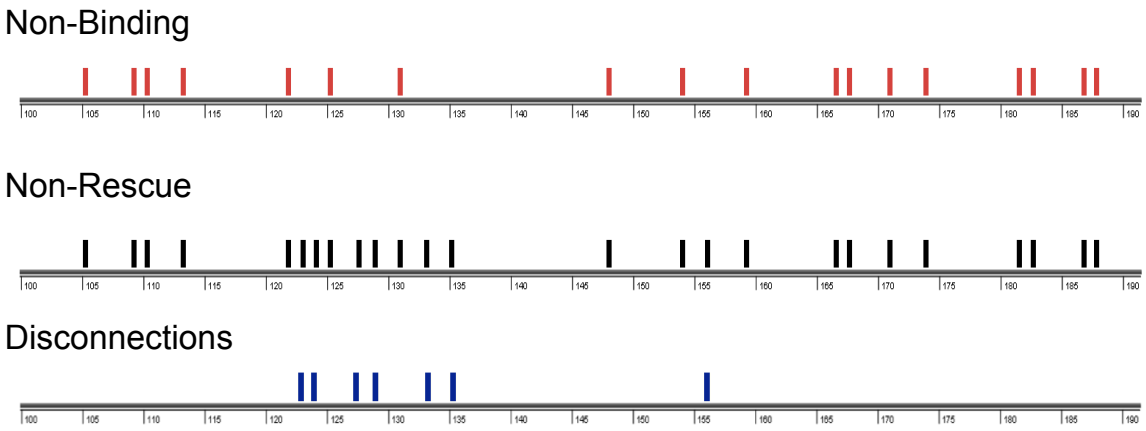

Figure 6 – Mapping of key E3 residues involved in pIC binding and rescue of ΔE3L in HeLa cells. Residues displaying loss of pIC binding, non-rescue of ΔE3L replication and disconnections between binding and rescue displayed. Amino acids position 100-190 shown.

3.3 Differential suppression of innate immune response by E3 mutants during infection

Following the evaluation of pIC binding and support of replication, 5 representative E3 mutants were selected to construct recombinant COP wild-type based viruses: Non-binding/non-rescue (NB/NR) mutants I110A and F159A; binding/non-rescue (B/NR) mutants N123A and F135A; binding/rescue (B/R) mutant C126A. Purity of viruses was confirmed by RT-PCR (Figure 7) of RNA extracted from infected BHK21 monolayers. Sequencing was also performed to confirm the presence of the desired mutations (data not shown). Purified recombinant viruses retained pIC binding (Figure 8A) and HeLa replication (Figure 8B) phenotypes. All viruses displayed expression of early viral genes (D12), while non-rescue mutants, I110A, N123A, F135 and F159A, were unable to produce intermediate proteins (G8).

Functional assays were performed on the mutants, assessing their activation of the innate immune responses and resistance to IFN. Activation of the innate immune response was assayed via phosphorylation of cellular PKR and eIF2a, and induction of pro-inflammatory cytokines IFN-β, TNF-α and IL-6. Retention of IFN resistance was evaluated by replication in Huh7R cells pretreated with IFN-β.

Activation of immune signaling proteins was evaluated 8 hpi in HeLa cells (Figure 9). Both total and phosphorylated PKR and eIF2a were evaluated by Western blotting. PKR and eIF2a phosphorylation levels were similar for cell control, COP-REV, and the B/R mutant C126A, while marked phosphorylation of

both PKR and eIF2a was observed in B/NR mutants (N123A, F135A) and NB/NR mutants (I110A, F159A) at levels similar to COP-ΔE3L infection. β-Actin levels were consistent in all samples.

Mutants were also assayed for induction of IFN-β, TNF-α and IL-6 transcription at 6 and 12 hpi by quantitative real-time (qRT) PCR (Figure 10A and 10B). IL-6 and TNF-α are induced by early viral products while IFN-β induction is associated with late viral products (Myskiw et al., 2009; Myskiw et al., 2011). Low levels of IFN-β, TNF-α and IL-6 induction were found for the B/R mutant C126A, which were comparable to COP-REV. At 12 hpi IFN-β was strongly induced, with the B/NR mutants N123A and F135A displaying greater inhibition than the NB/NR mutants I110A and F159A. In the case of IL-6 and TNF-α all non-rescue mutants were unable to inhibit induction.

Mutants were examined for replication in cells pre-treated with type 1 IFN (IFN-β1). COP-REV virus is known to be resistant to IFN-β pre-treatment, while COP-ΔE3L is unable to replicate in IFN-β pre-treated cells (Arsenio et al., 2008). All mutants, displayed similar titers 5 hpi independent of IFN-β pre-treatment (Figure 11A) serving as a baseline for virus replication. 24 hpi (Figure 11B), all non-rescue mutants (I110A, N123A, F135A and F159A) and displayed ≥2 log reduction in viral titer at ≥10U/ml of IFN-β pretreatment. Their titers similar to those observed at 5 hpi. Resistance to IFN-β pre-treatment was only observed in the B/R mutant C126A with inhibition of <0.5 log, analogous to that observed in COP-REV infection.

Figure 7 – RT-PCR confirmation of purified recombinant Copenhagen strain Vaccinia Virus I110A, N123A, C126A, F135A and F159A. Primers terminating on alanine substitution used to distinguish wild-type and mutant E3L constructs (Table 4). RNA extracted from confluent BHK21 monolayers infected at an MOI 1 collected after overnight growth.

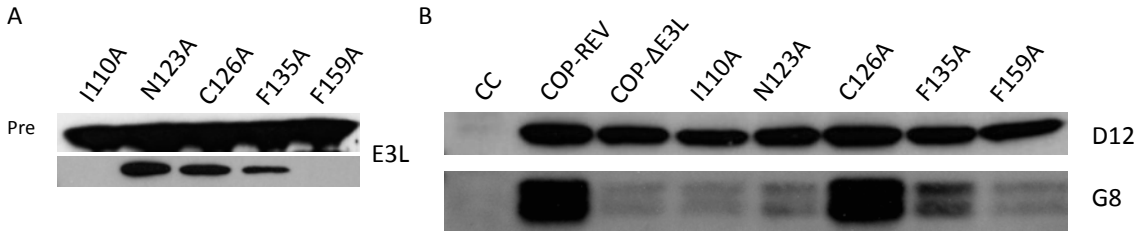

Figure 8 – Verification of dsRNA binding and replication phenotype in HeLa cells of recombinant I110A, N123A, C126A, F135A and F159A viruses. (a) pIC binding performed following MOI 1 infection in BHK21 cells after growth overnight. (b) HeLa replication evaluated by production of vvD12L (early) and vvG8R (late) proteins. HeLa monolayers at 80% confluency infected with an MOI of 2 and collected at 8 hpi.

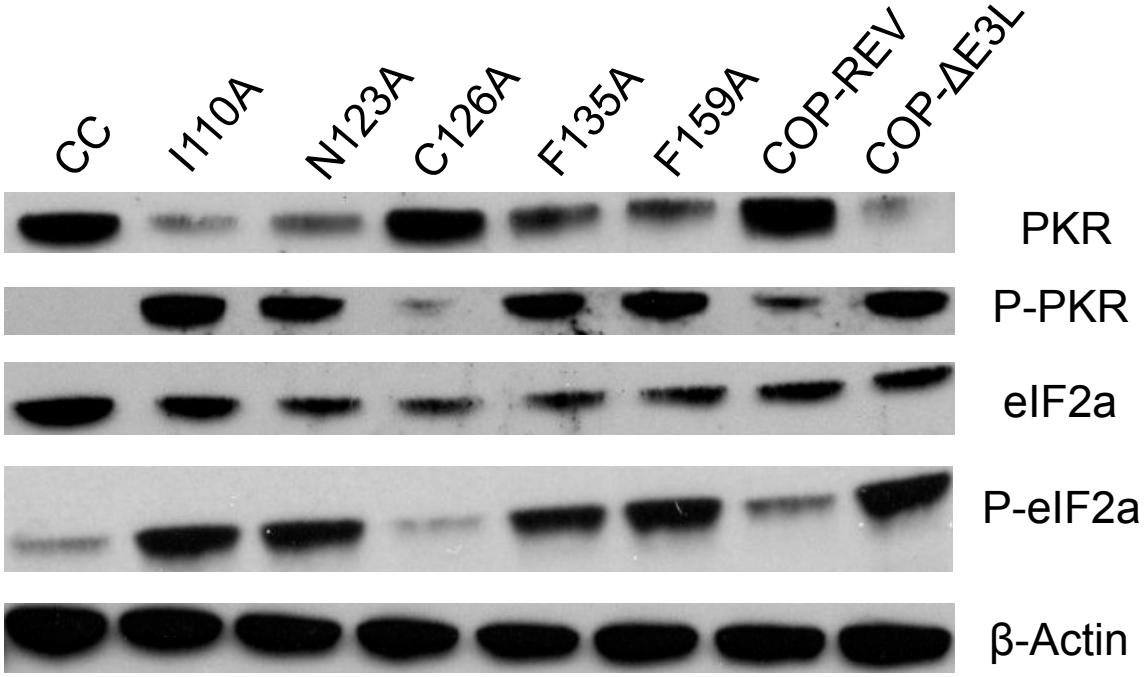

Figure 9 – Phosphorylation of PKR and eIF2a following infection with recombinant viruses. HeLa monolayers of 80% confluence were infected at an MOI of 2 and collected at 8 hpi. Western blotting was performed to detect total PKR, phosphorylated PKR (P446), total eIF2a, phosphorylated eIF2a and β-actin.

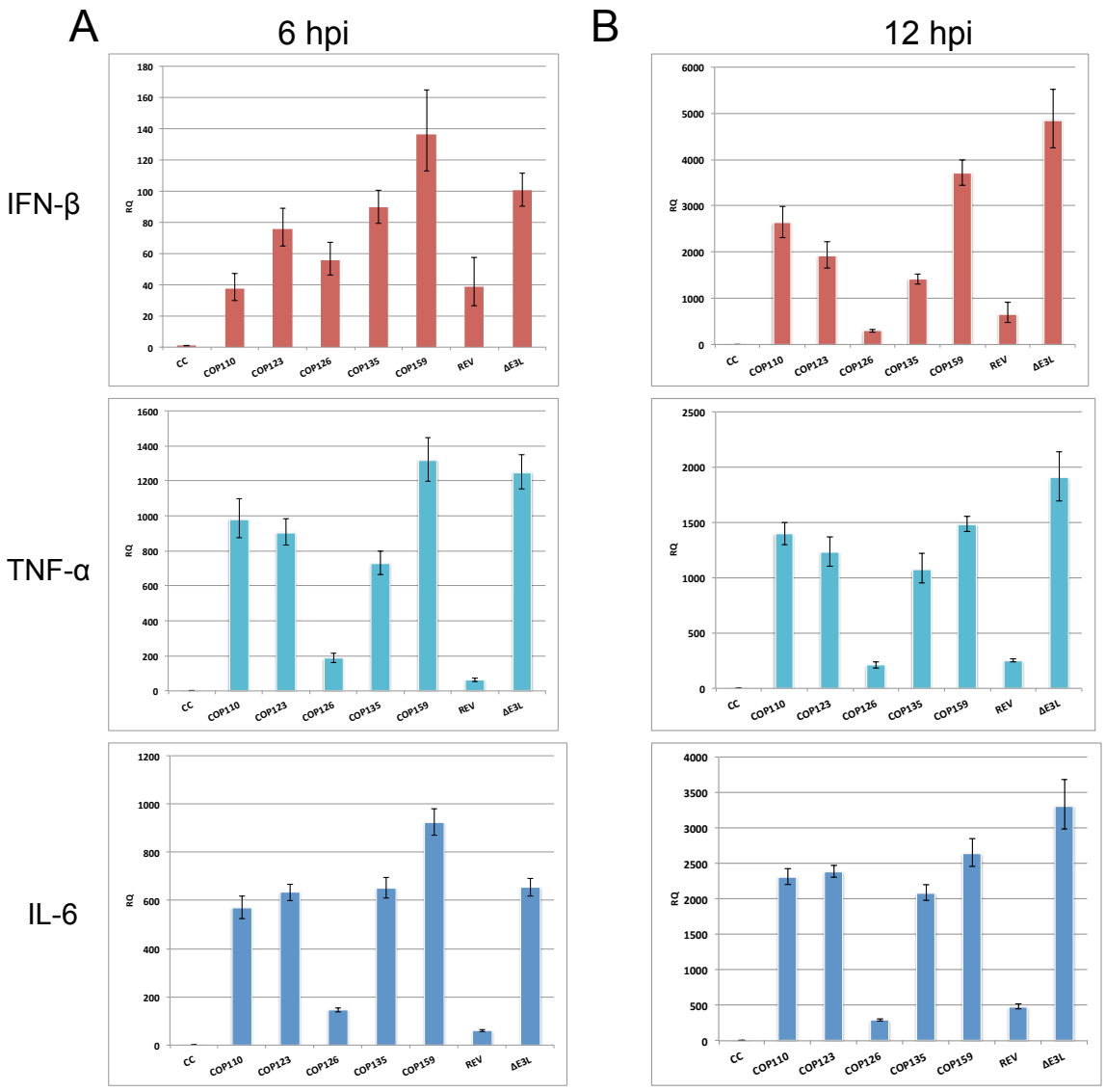

Figure 10 – Pro-inflammatory gene expression following infection with mutant viruses. IFN-β, TNF-α and IL-6 expression evaluated by qRT-PCR performed at (a) 6 and (b) 12 hpi using TaqMan probes and comparative CT analysis. HeLa monolayers of 80% confluence were infected at an MOI of 2, RNA collected at 6 and 12 hpi. Extracted RNA was reverse transcribed and 25 ng of cDNA was used for each reaction. PCR reactions performed in triplicate and normalized against human β-Actin in mock-infected wells. Error bars represent minimum and maximum RQ values.

A

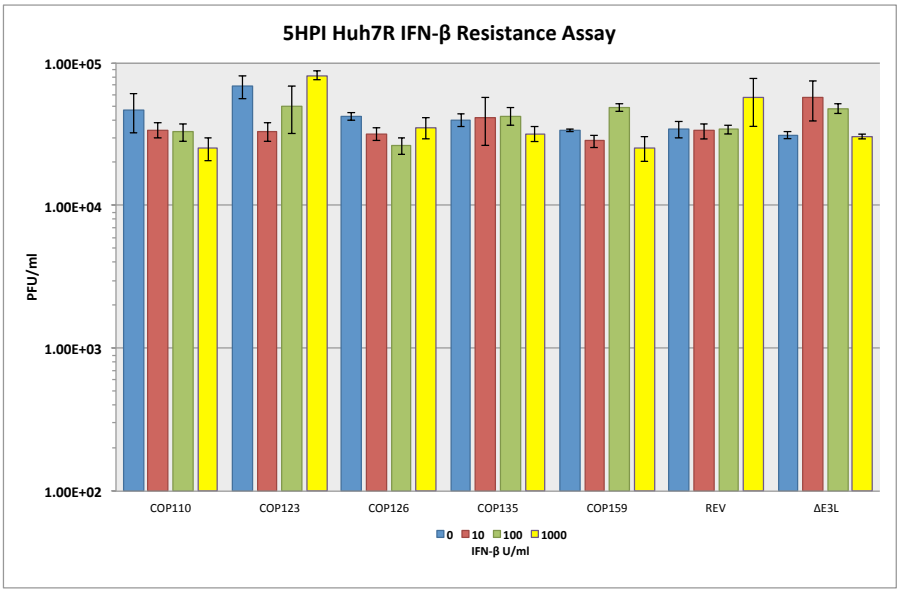

B

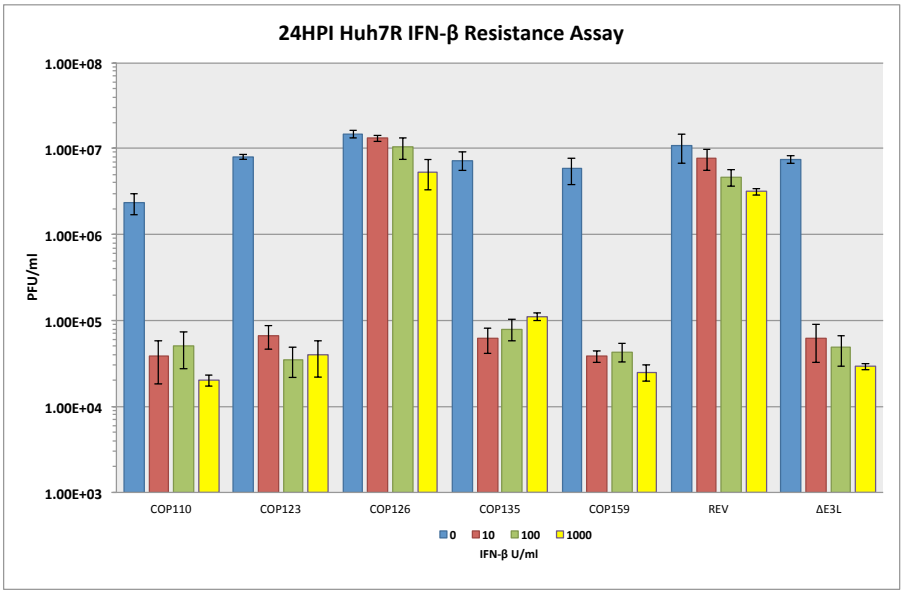

Figure 11 – Assay of viral replication in IFN-β pre-treated Huh7R cells. Huh7R monolayers of 80% confluence were pre-treated overnight with 0, 10, 100, or 1000 U/ml of IFN-β1. Monolayers were infected at an MOI of 1 with COP-REV, COP-ΔE3L, I110A, N123A, C126A, F135A or F159A viruses. Media was aspirated after 1 hr of infection and replaced with media of the previous IFN-β1concentrations. Monolayers were collected at (a) 5 and (b) 24 hpi. Titrations performed in triplicate using confluent BHK21 monolayers. Error bars represent standard deviation.

3.4 Protein-Protein Interaction of E3 mutants and Protein Kinase R

Differences in PKR interaction were explored between E3 mutants that display differential suppression of PKR following infection (Section 3.3). Truncation mutants expressed and evaluated for interaction with endogenous PKR in Huh7R (Figure 12A) and HeLa cell lines (Figure 12B). E3 mutants were expressed in Huh7R cells using recombinant viruses. Conversely, E3 mutants were expressed transiently using pJS5 in HeLa cells as the recombinant viruses grow differently in HeLa cells. In analysis of truncation mutants, PKR pulldown was observed only for full-length GST-E3L and the DRBD containing GST-C111 in both Huh7R and HeLa cells. COP-REV E3 protein was not present in pulldown samples, and neither COP-REV nor GST tag pulled-down endogenous PKR. Both virally expressed and transiently expressed GST mutants were able to pulldown PKR. Pre-pulldown levels were consistent for Huh7R infections, while variations in pre-pulldown protein concentration appear in HeLa cells. Following pulldown, GST-C111 levels were higher than other samples, though all were comparable in Huh7R and HeLa cells as analyzed by E3L and GST probing. Mutants transiently expressed in HeLa cells might compete for PKR binding with wild-type E3 due to COP-REV background.

Next, tagged single amino acid mutants were examined for their binding of endogenous PKR in HeLa cells (Figure 13). GST tagged F159A displayed reduced binding in comparison to other mutants, while the negative control GST-Δ175, was

unable to bind PKR. Thus, all tagged E3 alanine mutants, irrelevant of dsRNA binding and host range, were able to able to pulldown endogenous PKR although the truncated GST-Δ175 did not.

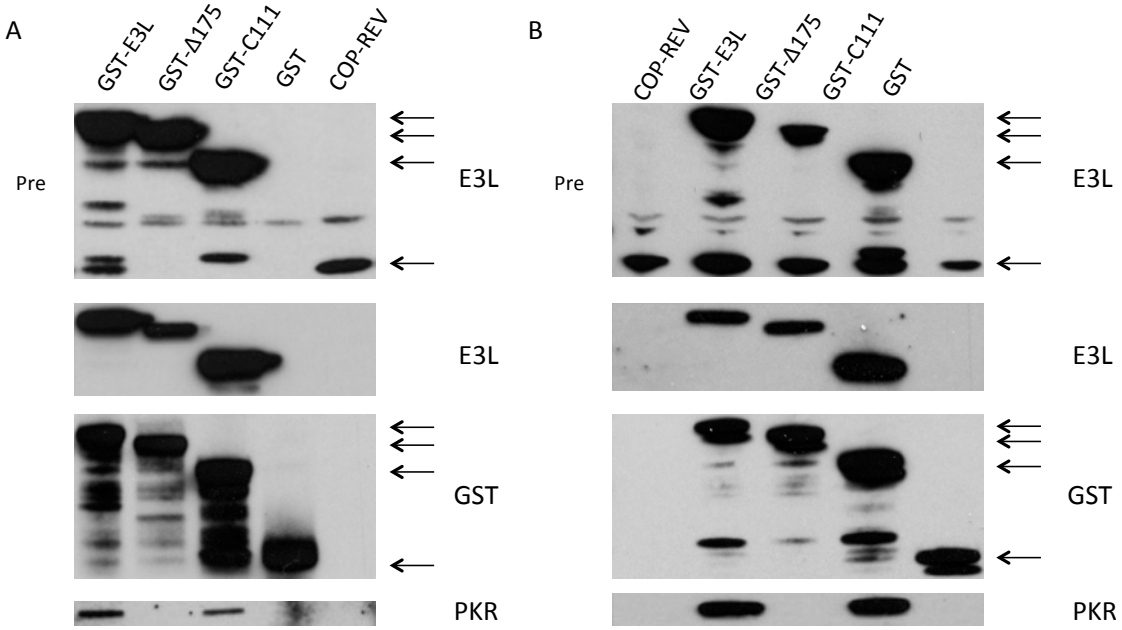

Figure 12 – Differential glutathione-pulldown of endogenous PKR by E3 truncation mutants. (A) Pulldown of PKR in Huh7R cells by E3 mutants expressed virally at an MOI of 2, samples collected 8 hpi. (B) Pulldown of PKR in HeLa cells, transiently expressed GST and tagged mutants in a MOI 2 COP-REV background, collected 10 hpi. HeLa monolayers of 80% confluence were transfected with pJS5 constructs of GST-E3L, GST-Δ175, GST-ΔC111 or GST for 2 hrs prior to infection. Samples collected under non-denaturing conditions and precipitated with Glutathione beads. Pre-pulldown samples were collected in 1xSDS buffer. Samples probed with GST, vvE3L #1/#2 and total PKR antibodies.

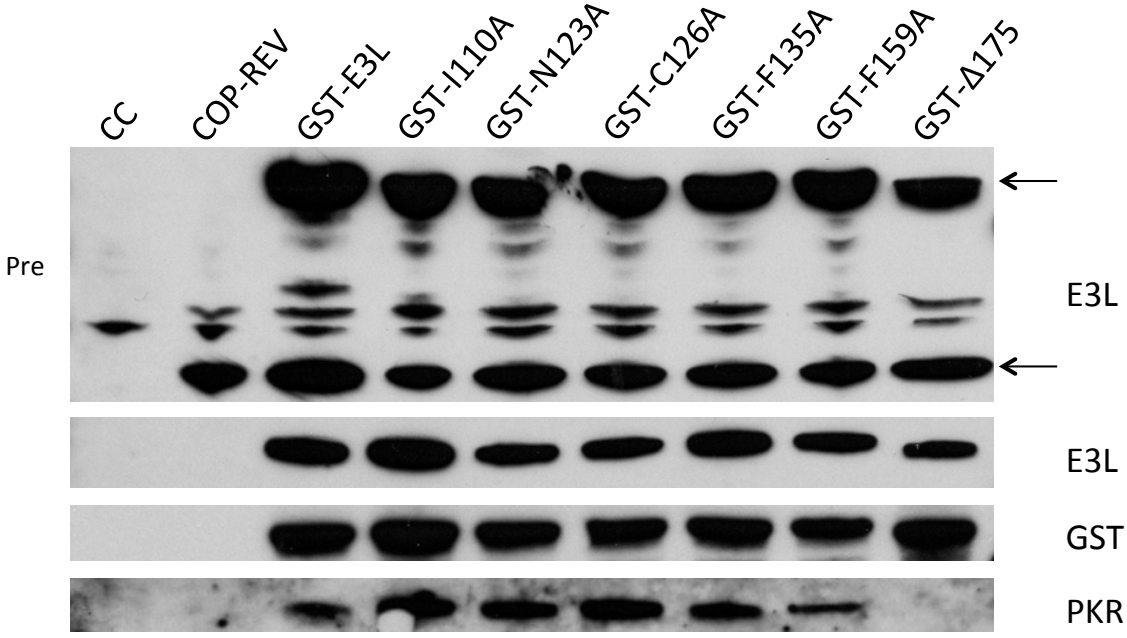

Figure 13 – Glutathione-pulldown of PKR by E3 single amino acid mutants. HeLa monolayers grown to 80% confluence were transfected with pJS5 constructs expressing GST-E3L, GST-110, GST-123, GST-126, GST-135 or GST-159 for 2 hrs prior to infection with COP-REV at an MOI of 2. Infections were collected under non-denaturing conditions 10 hpi and precipitated with Glutathione beads. Pre-pulldown samples were collected in 1xSDS buffer for Western blotting. Samples probed with GST, vvE3L #1/#2 and total PKR antibodies.

3.5 Analysis of E3 protein-protein interactions by 2D Differential Gel Electrophoresis and Mass Spectroscopy

Novel PPIs between E3 mutants and HeLa proteins were explored by 2D DIGE and MS/MS analysis. Lysates obtained from Glutathione pulldowns of E3 truncation mutants and GST tag control was utilized. Lysates from HeLa cells were initially analyzed for proteome differences via silver staining (Figure 14). Banding patterns differed between mutants, with GST-E3L and GST-C111 showing similarities. Further analysis was performed using 2 CyDye 2D gels, comparing pairs of lysates: (A) GST-E3L vs. (B) GST-Δ175, (A) GST-E3L vs. (C) GST-C111 and (A) GST-E3L vs. (D) GST alone (Figure 15). Spots identified by peptide mass fingerprint (PMF) and/or MS/MS sequencing circled. Top matches displayed in Table 8, along with lysate association, GenBank number and identification scores. E3L mutants were confirmed in spot 7 (GST-E3L), 9 (GST-Δ175) and 26 (GST-C111), as well as a number of spots were identified as GST tag variants. Vimentin and Keratin, common contaminants, were identified in most gels. Confirmation of differential interaction with LANCL1, EEF1B, EF1A1 and Cbr1 was attempted by Western blotting, but was inconclusive, due to antibody cross-reactivity (Appendix 3).

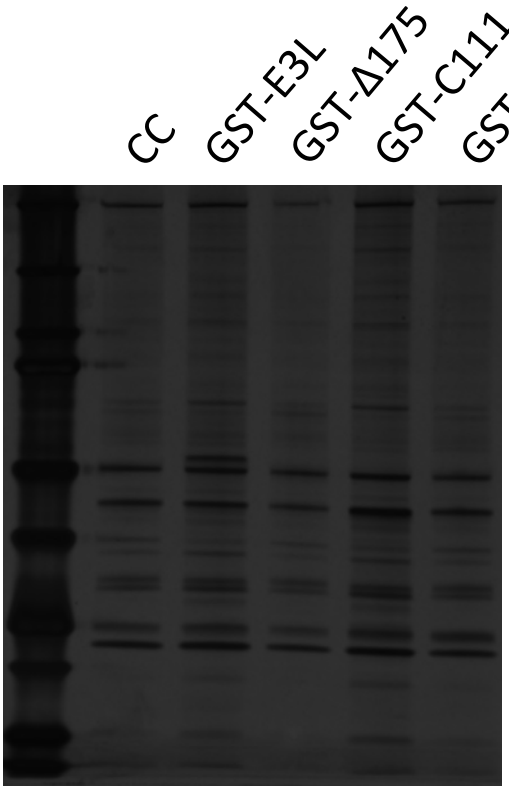

Figure 14 – Silver staining of glutathione-pulldowns reveals significant differences in protein interaction profiles. HeLa monolayers grown in 100 mm dishes transfected with pJS5 constructs expressing GST-E3L, GST-Δ175, GST-C111 or GST for 4hrs prior to infection with COP-REV at an MOI of 2. Collected under non-denaturing conditions 8 hpi for glutathione-pulldown.

A / B

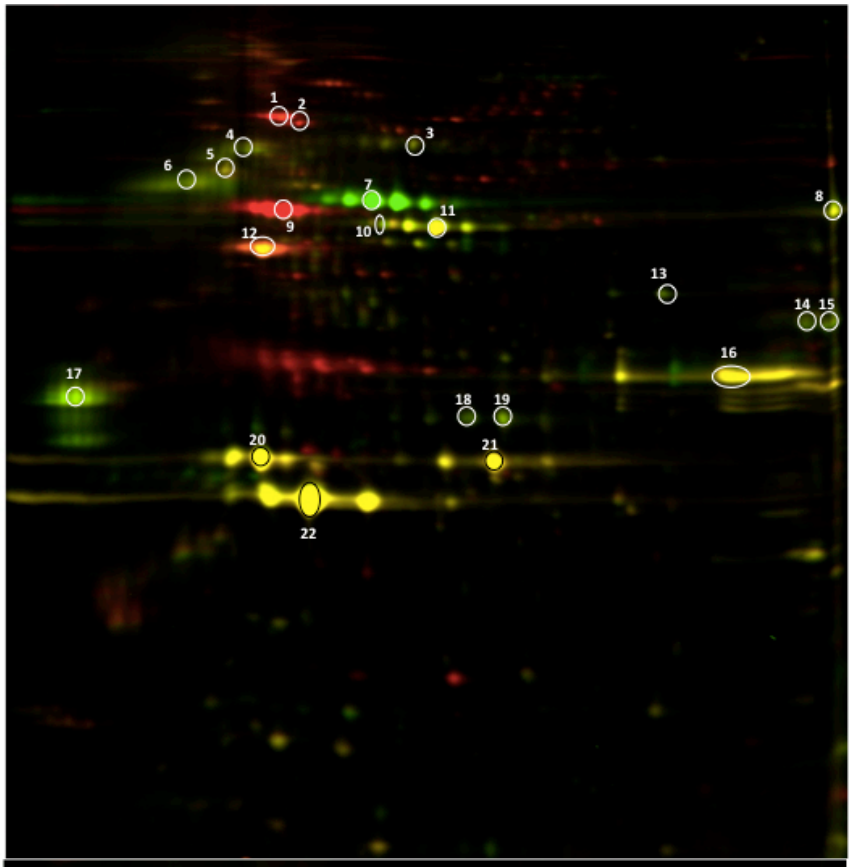
1
2
3
4
5
6
7
8
9
10
11
12
13
14
15
16
17
18
19
20
21
22

A / C

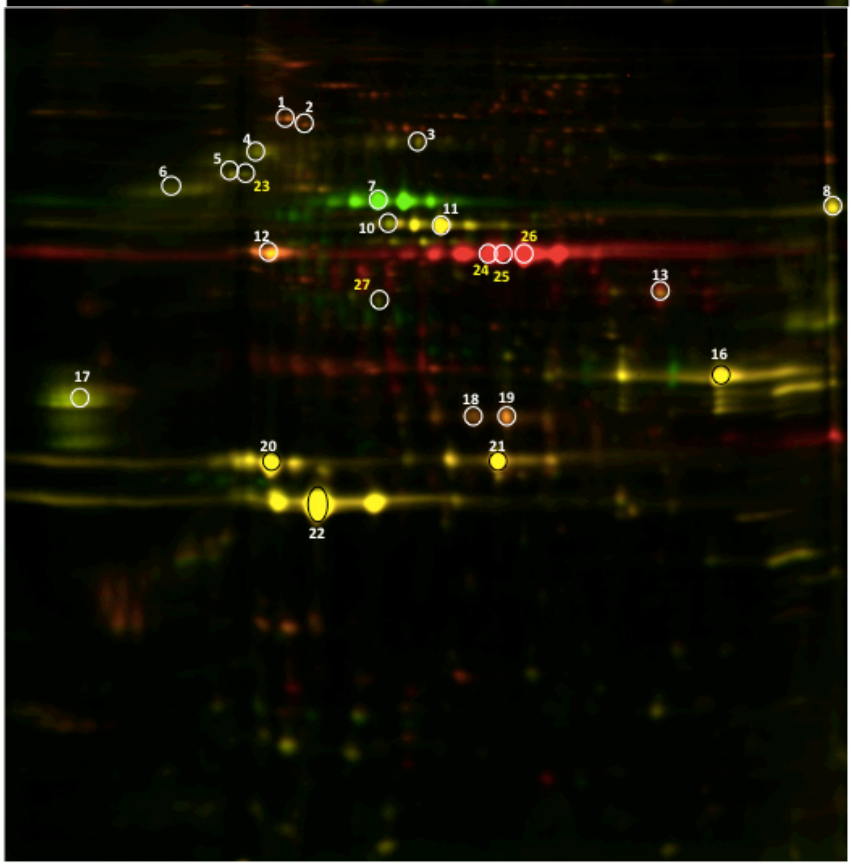
1
2
3
4
5
6
7
8
10
11
12
13
16
17
18
19
20
21
22
23
24
25
26
27

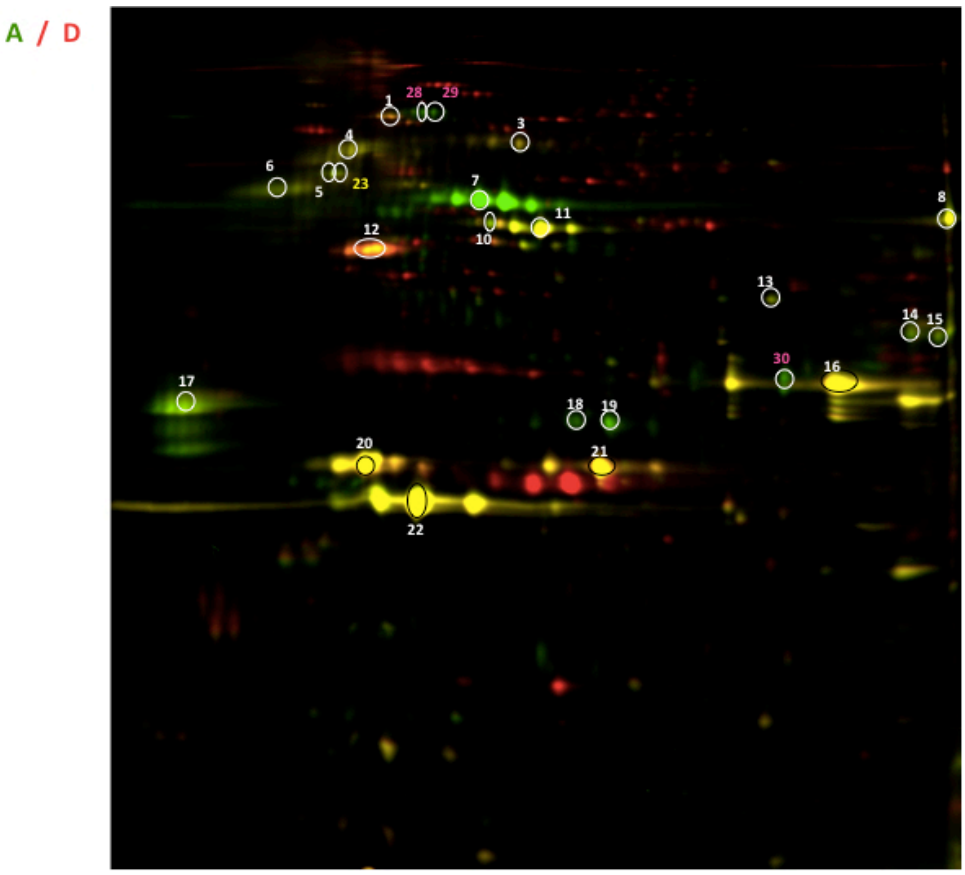

Figure 15 - Overlays of 2D DIGE 2 CyDye Analysis. (A) GST-E3L vs. (B) GST-Δ175, (A) GST-E3L vs. (C) GST-C111 and (A) GST-E3L vs. (D) GST alone. Spots picked for identification numbered by vertical position. HeLa monolayers of 80% confluence transfected with pJS5 expressing GST-E3L, GST-Δ175, GST-C111 or GST with COP-REV background at an MOI of 2. Infections were collected under non-denaturing conditions 8 hpi and precipitated with Glutathione beads.

#	Identification	Conf	Score	C.I.%	Association	GenBank
1	E3L	None	13	71	All	N/A
2	Heat Shock Protein 70 kDa	Hi	104	100	GST-Δ175, GST-C111	gi|386785
3	GST Tag	None	8	12	All	N/A
4	Keratin type 1 cytoskeletal 9	Hi	111	100	GST-E3L, GST-Δ175	gi|55956899
5	Vimentin	Hi	92	100	GST-E3L, GST-Δ175	gi|47115317
6	Keratin Type 1 cytoskeletal 10	Hi	96	100	GST-E3L	gi|269849769
7	E3L	Hi	44	100	GST-E3L	N/A
8	Elongation Factor 1-α-1 (*Cycotella cryptica*)	HI	86	97	All	gi|59859756
9	E3L	Hi	66	100	GST-Δ175	N/A
10	Elongation Factor 1-γ	Hi	265	100	GST-E3L	gi|39644794
11	Elongation Factor 1-γ	Hi	162	100	All	gi|39644794
12	β-Actin	Hi	208	100	All	gi|14250401
13	LanC-like Protein 1	Hi	80	100	GST-E3L, GST-C111	gi|49456511
14	Zinc finger CCCH-type	Low	63	89	GST-E3L	gi|119625810
15	Translation Elongation Factor 1-α-1	Hi	80	100	GST-E3L	gi|15277711
16	Chain A, Human Cbr1 in complex with Hydroxy-Pp	Hi	297	100	All	gi|66360348
17	Elongation Factor 1-β	Hi	143	100	GST-E3L, GST-C111	gi|4503477
18	GST Tag	Hi	49	100	GST-E3L	N/A
19	Carbonyl Reductase 1	Hi	66	100	GST-E3L	gi|4502599
20	Chain B, Ligand free heterodimeric GST	Hi	299	100	All	gi|5822511
21	Chain A, Ligand free GST	Hi	213	100	All	gi|4388890
22	GST Tag	Hi	370	100	All	N/A
23	Vimentin	Hi	182	100	GST-E3L, GST-C111	gi|47115317
24	GST Tag	Hi	83	100	GST-C111	N/A
25	GST Tag	Hi	115	100	GST-C111	N/A
26	GST Tag E3L	Hi Low	118 72	100 -	GST-C111	N/A
27	hCG2041303	None	53	-	GST-E3L	gi|119607302
28	RAD9 Homolog	None	44	-	GST-E3L	gi|15928780
29	Immunoglobulin Heavy Chain Var Region	None	40	-	GST-E3L	gi|14210303
30	Carbonyl Reductase 1	Hi	68	96	GST-E3L	gi|4502599

Table 8 - Identification of proteins interacting with GST-E3L, GST-Δ175, GST-C111 and GST in a COP-REV infection context. MS Data analysis performed with MASCOT on PMF and MS/MS data generated by MALDI TOF/TOF analysis. Data analysis performed by Applied Biomics using NCBinr database including Vaccinia COP genome and GST tag sequences. Confidence interval of identification, protein scores, lysate association and GenBank number indicated.

4.0 Discussion

The double-stranded RNA binding domain of Vaccinia E3 protein is thought to be largely responsible for the innate immune suppressive features of this protein *in vitro* (Langland and Jacobs, 2004). This study marks the first full mutational analysis of this domain and correlation of dsRNA binding with host range function. PKR suppression is seen as a major role of E3, models proposed involved sequestering of dsRNA and/or PKR dimerization inhibition through PPIs (Romano et al., 1998). Here, suppression of PKR by E3 was found to be independent of dsRNA binding or PKR interaction. These features were investigated through use of purified mutant viruses with differing binding and host range phenotypes. These viruses were also used to investigate correlations with IFN resistance and cytokine suppression in response to infection. Both features displayed strong correlation with HeLa replication competence, rather than dsRNA binding. Lastly, the PPIs of E3 were explored, elucidating novel interactions with host elongation and metabolic factors.

Preservation of E3 mutants' dsRNA binding was examined using pIC bead pulldowns in an infection context for all mutants. In this analysis, all mutant E3 proteins were expressed to similar levels and binding/non-binding displayed a largely binary pattern. All non-binding mutants were involved mutation of highly conserved residues (Table 5). All low conservation residues bound pIC, although E138A displayed reduced binding (Appendix 2B). Minor migration differences

were noted in several glutamic acid and aspartic acid mutants (D86A/D87A, D87A, E91A, E96A, D97A), potentially related to charge alteration. Thus, our study found 18 E3 residues involved in dsRNA binding, expanding on the 6 residues previously mapped (Figure 6) (Ho and Shuman, 1996b). Important residues previously discovered largely correlate with this analysis. Previous mutational analysis of E3L based on *E. coli* and *D.* melanogaster DRBDs reveal the importance of residues K167 and R168 in dsRNA binding and PKR suppression, these mutants were unable to bind pIC in this study (Romano et al., 1998). Previous alanine scanning mutagenesis of 14 residues demonstrated reduced dsRNA binding of E124A, F135A, F148A, K167A, R168A and K171A (Ho and Shuman, 1996b). All binding residues found previously were replicated in our study; however, E124A was found to bind pIC in all trials. This difference may be accounted for by the protein extractions techniques utilized and method of dsRNA binding analysis. In the previous study, proteins were expressed in *E. coli* and extracted in high salt, attached to a membrane and re-natured for analysis with radioactive dsRNA probes. This re-naturation process may not allow proper protein folding to occur leading to loss of dsRNA binding. Conversely, in this study proteins were expressed in HeLa cells and extracted under non-denaturing conditions, retaining their native form and assayed for binding via pIC beads.

The second dimension of mutant analysis was support of Vaccinia ΔE3L virus replication in HeLa cells. The deletion of E3L is known to restrict the host range of Vaccinia, limiting replication in HeLa cells (Beattie et al., 1996), blocking

replication at intermediate gene translation with strong induction of OAS and PKR (Ludwig et al., 2006). Using plasmids bearing the flanking regions of the Thymidine Kinase locus (pJS5), the mutant E3L genes were inserted into COP-ΔE3L virus bearing EGFP for fast fluorescent identification of replication. The recombinants were passaged in HeLa monolayers 3 times and plaque formation assayed. Similar to the binding assays, a gradient of replication was not observed, with 25 mutants unable to support replication. However, mutants D103A and L182A displayed limited replication (Table 5). As L182 represents the first residue of a leucine repeat, both L183A and L182/L183A mutants lacking replication, some alteration of PPI may be occurring. Alternatively, D103A bound pIC and its importance has not previously been described, however, aspartic acid mutation may alter secondary structure, thus altering E3 properties. All mutants supporting ΔE3L replication were found to bind pIC, supporting dsRNA binding as an essential feature in E3 function (Table 6). Nonetheless, 7 mutants were found to lack replication in HeLa cells despite binding of pIC: N123A, E124A, Q127A, T129A, W133A, F135A and G156A (Table 7). Six of these residues cluster in the region of 123-135, Figure 6, indicating a potential motif; unfortunately the structure of the DRBD has not been determined, disallowing structural analysis of this region. Based on these rescue assays, a disconnection was found between dsRNA binding by E3 and host range function.

As pIC is a synthetic analog of dsRNA, concerns may be raised to its use in studying viral dsRNA binding. However, pIC use is well established, having been

used in previous studies of DRBPs such as E3 (Chang et al., 1992)(Ho and Shuman, 1996a), PKR (O'Malley et al., 1986), RIG-I (Yoneyama et al., 2004), and viral DRBP VP35 and NS1 (Hale et al., 2010; Prins et al., 2010), all of which have also been shown to bind dsRNA. Poly I:C has also been shown to compete with radiolabeled dsRNA for E3L binding (Ho and Shuman, 1996a) and activate RIG-I and PKR pathways associated with dsRNA presence (Silva et al., 2004; Yoneyama et al., 2005). Thus, pIC appears to bind analogously to dsRNA, and stimulate dsRNA associated host responses.

In order to better understand the alterations to the innate immune responses by E3, representative viruses displaying different pIC binding and rescue phenotypes were generated based on the above assays, to analyze correlations with known E3 features: 2 non-binding/non-rescue (NB/NR) mutants I110A and F159A; 2 binding/non-rescue (B/NR) mutants N123A and F135A; 1 binding/rescue (B/R) mutant C126A. In these recombinant viruses the wild-type E3L locus was replaced with a mutant gene. EGFP was also inserted to assist in purification and assessment of replication. Viral purity (Figure 7), retention of pIC binding (Figure 8A) and HeLa replication phenotype (Figures 7B) were verified. Confirmation of interaction with viral dsRNA was attempted through use of GST fusion mutants and RNA extraction following pulldown as outlined in Section 2.7.3. Unfortunately, non-specific binding of dsRNA and DNA to immobilized glutathione was found, confounding assessment of viral dsRNA interaction (date not shown). Hence, these

5 E3 mutants were utilized to explore alterations in PKR activation and interaction as well as innate immune activation in response to infection.

PKR suppression is seen as a major role of E3, thus effects on the classical PKR-eIF2a pathway were explored between purified mutants. In this pathway, PKR is activated in a dsRNA dependent manner, resulting in dimerization and phosphorylation at T446, leading to eIF2A phosphorylation at Ser51, which inhibiting translation initiation (Section 1.2.5) (Garcia et al., 2006). It would be expected that pIC binding mutants N123A, C126A and F135A would display similar PKR inhibiting characteristics, through sequestering dsRNA. Surprisingly, only the B/R mutant C126A was capable of suppressing PKR and eIF2a phosphorylation (Figure 9), all non-rescue mutants displaying phosphorylation levels comparable to ΔE3L. Previously, mutants demonstrating loss of dsRNA binding were correlated with loss of PKR suppression (Chang and Jacobs, 1993). However, in this study non-rescue mutants both lacking dsRNA binding, I110A and F159A, and retaining dsRNA binding, N123A and F135A, led to PKR activation. These results do not support a simple dsRNA sequestering model in suppression of PKR (Figure 16A).

An alternative model of PKR suppression is based on PKR-E3 interaction requiring residues W66, K167 and R168 (Romano et al., 1998). In order to test this model N-terminal GST fusions of E3L, E3L-Δ175, E3L-C111, I110A, N123A, C126A, F135A and F159A were generated for transient expression. Additionally, recombinant viruses expressing GST tagged E3L, E3L-Δ175, E3L-C111 or GST were

constructed. These tagged mutants were used to pulldown endogenous PKR in both Huh7R and HeLa cells. Virally expressed GST-E3L and GST-C111 bound PKR in Huh7R and HeLa cells, Figures 11A and 11B, while GST-Δ175 and GST alone lacked this interaction. Viral expression in HeLa cells was attempted, however, GST-Δ175 and GST virus replication was inhibited. In the case of endogenous PKR pulldown in Huh7R cells it appears GST-E3L shows greater affinity for PKR than GST-C111 (Figure 12A). This lower affinity may be accounted for by absence the ZBD bearing W66 in GST-C111, its importance in PKR interaction previously demonstrated (Romano et al., 1998). Exploring the interaction model of PKR suppression, Figure 13, tagged alanine mutants were expressed transiently in HeLa cells. Interaction of all 5 alanine mutants with PKR was demonstrated at a similar level to wild-type E3, while controls and GST-Δ175 displayed no interaction. Retention of PKR-E3 interactions by these mutants sheds new light on the model of PKR suppression. In these experiments PKR interaction was demonstrated with E3 mutants capable and incapable of PKR suppression, revealing the inadequacy of the interaction inhibition model, Figure 16B. Figure 16C displays a proposed model of PKR-E3 suppression, "X" indicating an adaptor protein or inhibition of a PKR activation pathway. Thus, PKR-E3 interaction is associated with suppression, but potential adaptor proteins or inhibition of non-dsRNA pathways may be involved. These interaction assays also support the ability of E3 bind cytoplasmic PKR in a non-dsRNA dependent manner, as NB/NR mutants I110A and F159A retained PKR interaction, in agreement with previous *in vitro* analysis (Sharp et al.,

1998). Interestingly, no wild-type E3 from the COP-REV background was pulled down during transient expression of GST fusion mutants, indicating a lack of E3 protein heterodimer/oligomer formation. On an alternative interpretation of the results, B/NR mutants N123A and F135A may have altered dsRNA specificity, accounting for their B/NR phenotype. Exploration of this view was regrettably unsuccessful, the structure and specificity of viral dsRNA interacting with E3 remains unknown at present.

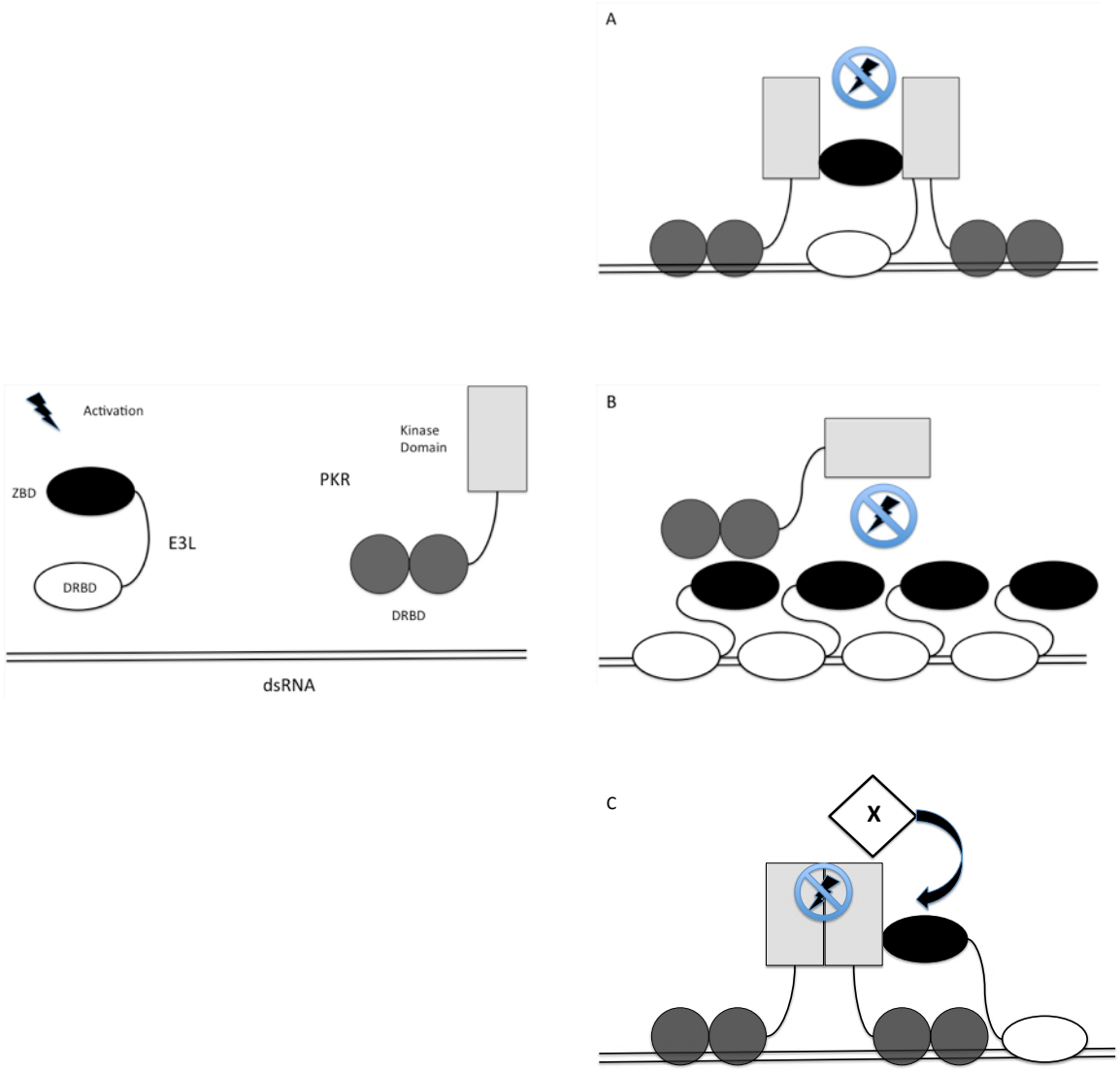

Figure 16 – Proposed models of PKR-E3 interaction. Classical models of E3 based PKR suppression, (A) interaction of E3L with PKR prevents dimerization and (B) sequestering of dsRNA by E3. (C) Proposed model, E3 interacting with PKR and dsRNA, but suppression is adaptor or upstream suppression "X" related. E3: Z-DNA binding domain (black) and dsRNA binding domain (white). PKR: kinase domain (light grey) and dsRNA binding domain (dark grey). Classical models based on models proposed by Romano and Heinicke (Heinicke et al., 2011; Romano et al., 1998).

The 5 recombinant viruses were also used to investigate IFN resistance and cytokine suppression. These features were explored to elucidate innate pathways altered in response to infection by Vaccinia bearing E3 B/R, B/NR and NB/NR phenotypes. Both PKR dependent and independent pathways were explored as activation on ΔE3L infection has previously been demonstrated (Myskiw et al., 2009). Inhibition of ΔE3L virus replication of in IFN stimulated Huh7R cells has been shown to be largely PKR dependent, despite the stimulation of multiple ISGs on IFN treatment (Arsenio et al., 2008). Analysis of mutant replication in IFN-β pre-treated Huh7R cells, Figure 11A and 11B, revealed IFN sensitivity in all non-rescue mutants, I110A, N123A, F135A and F159A, independent of dsRNA binding phenotype. This replication inhibition following ≥10U/ml IFN-β pre-treatment was analogous to that observed in ΔE3L virus, titers remaining unchanged between 5 and 24 hpi. These finding supports an alternative model of PKR binding, Figure 16C, as B/NR mutants N123A and F135A on the sequestering model should have possessed IFN resistance. The inhibition of non-rescue viruses was expected based on observed PKR activation in HeLa cells following infection and PKR-related ΔE3L inhibition in IFN stimulated Huh7R cells (Figure 9).

A second avenue of host response to infection, cytokine induction following PRR detection, was explored through qRT-PCR. The cytokines induced by both PKR dependent and independent pathways in response to infection were studied, focusing on IFN-β, TNF-α and IL-6 at 6 and 12 hpi. IFN-β can be stimulated via RIG-I or PKR activation through IRF3/7, and is associated with late viral RNA

PAMPs. Conversely, TNF-α and IL-6 are associated with early viral PAMPs, their activation PKR dependent and independent, respectively (Myskiw et al., 2009; 2011). Strong induction of all cytokines was observed in non-rescue mutants I110A, N123A, F135A and F159A at 12 hpi, indicating the independence of dsRNA binding and cytokine suppression. IFN-β induction increased >20 fold between 6 and 12 hpi, in accordance with its previous association with late PAMPs. Furthermore, some inhibition of IFN-β was present for B/NR mutants, N123A and F135A at 12 hpi, demonstrating possible specificity for late viral PAMPs. However, neither of these mutants demonstrated significant inhibition of TNF-α or IL-6. In this study, the F159A mutant virus demonstrated the greatest induction, and displays altered cellular localization, the basis of this requiring further study (data not shown). Thus, E3 suppresses both PKR dependent and PKR independent pathways. Moreover, IFN resistance and cytokine induction display strong correlations with host range function in HeLa cells, rather than dsRNA binding as would be expected based on previous work (Chang and Jacobs, 1993). In order to better understand the mechanisms of E3 suppression, a clearer picture of its partners during infection is required.

To better understand the role of E3 during infection, a proteomic approach was taken, pairing 2D gel analysis with mass spectroscopy (MS). Previous PPI studies have been performed using Yeast two-hybrid methods (Van Vliet et al., 2009). Here, GST tagged E3 and truncation mutants with well-defined phenotypes, GST-E3L, GST-Δ175 and GST-C111 were used to pulldown HeLa proteins in an

infection context. The use of DIGE in an infection context allows potential detection E3 PPIs with other viral proteins, a possibility not realizable in previous studies. These pulldowns were compared in pairwise fashion to illuminate differential PPIs. Significant protein differences were noted in gel overlays, Figure 15, and thirty PPIs identified through MS analysis (Table 8). Interaction patterns were common between GST-E3L and the GST-C111 truncation, as expected due to comparable *in vitro* phenotypes and replication competence in HeLa cells. Only a single immune factor was identified, LanC-like protein 1 (LANCL1), a protein involved in anti-microbial peptide synthesis, was associated with both GST-E3L and GST-C111. Interaction with PKR was not observed, and was missing in the previous Yeast two-hybrid analysis. Unexpectedly, high confidence identification of interaction with translation factors was observed, GST-E3L and GST-C111 binding Elongation Factor 1 B, while GST-E3L pulled down Eukaryotic Elongation Factor 1-α-1 (EEF1A1) and Translation Elongation Factor 1 gamma (EEF1G). Stress related heat-shock protein 70 kDa was not found to associate with GST-E3L, however, it was found in both GST-Δ175 and GST-C111 pulldowns, indicating potential interaction with this pathway by the truncation mutants. A number of interactions with Carbonyl Reductase 1 (Cbr1), involved in NADPH metabolism were also found. Verification of PPI with Cbr1, EEF1A1, EEF1G and LANCL1 were attempted using lysates assayed for PKR interaction in Figure 12. Unfortunately, these interactions could not be verified, in part due to antibody cross-reactivity in the case of EEF1A1 (Appendix 3). This approach, though it allows the comparison

of PPIs of multiple samples on a single gel, has significant shortcomings. Firstly, CyDye labels are attached to lysine residues, thus proteins lacking or enriched in lysines will not label properly. Secondly, large >150 kDa and small <10 kDa proteins are difficult to resolve and reproducibility between trials is an issue (Timms and Cramer, 2008). Additionally, proteins with isoelectric points outside the pH range chosen for analysis will not be captured. Finally, protein spots may contain multiple proteins, thus MS analysis is not guaranteed to identify the protein differentially expressed (Brewis and Brennan, 2010). Currently, the importance of the factors identified by 2D DIGE remains open, requiring further investigation.

5.0 Conclusion

The Vaccinia virus E3 protein produced early in infection is known to bind dsRNA produced by viral transcription and suppress cytokine signaling through PKR-dependent and independent pathways. In this study alanine scanning mutagenesis was performed on all amino acids of the dsRNA binding domain. These mutants were expressed in an infection context and tested for retention of dsRNA binding and support of Vaccinia ΔE3L replication in HeLa cells. Through this analysis correlations were found between the ability to replicate in HeLa cells and dsRNA binding, indicating a potential role of binding as a 'targeting' feature of E3 allowing immune suppression. However, 7 dsRNA binding, non-rescue mutants were found, indicating a disconnection between these features of E3. Differences in PKR activation and interaction, cytokine signaling and Type I IFN resistance were investigated through construction of 5 recombinant Vaccinia viruses bearing I110A, N123A, C126A, F135A and F159A mutations. These investigations demonstrated a strong correlation between non-rescue phenotypes and PKR activation. The independence of PKR binding from suppression was also revealed through glutathione pulldown studies. These findings also reveal the need for refinement of the PKR-E3 interaction model. Furthermore, corresponding correlations were found on investigation of PKR dependent and independent cytokine induction, with HeLa replication phenotype, not dsRNA binding correlating with suppression. Poly I:C binding, non-rescue mutants did however demonstrate partial inhibition of IFN-

β at 12 hpi, suggesting specificity for this pathway. Largely PKR dependent replication in IFN-β pre-treated Huh7R cells also displayed association with rescue phenotype, rather than dsRNA binding.

In summary, these investigations of innate immune activation demonstrate the insufficiency of both current PKR-E3 models, and a significant role beyond dsRNA sequestering and PKR suppression for E3. Novel protein-protein interactions were discovered between E3 and host elongation and metabolic factors. This research represents the first full mapping of key amino acids in the DRBD of E3 involved in dsRNA binding and host range. Paired with the analysis of specific residues, this study provides novel insights into E3's mechanism of suppressing immune responses and forms a basis for future investigations of this important host range factor and other double-stranded RNA binding proteins.

References

Abcam. 2011. “Immunoprecipitation protocol.” *Technical Resources*: http://www.abcam.com/technical

Alcami, A., Symons, J.A., Smith, G.L., 2000. The vaccinia virus soluble alpha/beta interferon (IFN) receptor binds to the cell surface and protects cells from the antiviral effects of IFN. J. Virol. 74(23), 11230–11239.

Arsenio, J., Deschambault, Y., Cao, J., 2008. Antagonizing activity of vaccinia virus E3L against human interferons in Huh7 cells. Virology. 377(1), 124–132.

Bandi, P., Pagliaccetti, N.E., Robek, M.D., 2010. Inhibition of type III interferon activity by orthopoxvirus immunomodulatory proteins. Journal of Interferon & Cytokine Research. 30(3), 123–134.

Barral, P.M., Sarkar, D., Su, Z.-Z., Barber, G.N., DeSalle, R., Racaniello, V.R., Fisher, P.B., 2009. Functions of the cytoplasmic RNA sensors RIG-I and MDA-5: key regulators of innate immunity. Pharmacol. Ther. 124(2), 219–234.

Basler, C.F., Amarasinghe, G.K., 2009. Evasion of interferon responses by Ebola and Marburg viruses. Journal of Interferon & Cytokine Research. 29(9), 511–520.

Beattie, E., Paoletti, E., Tartaglia, J., 1995. Distinct patterns of IFN sensitivity observed in cells infected with vaccinia K3L- and E3L- mutant viruses. Virology. 210(2), 254–263.

Beattie, E., Kauffman, E.B., Martinez, H., Perkus, M.E., Jacobs, B.L., Paoletti, E., Tartaglia, J., 1996. Host-range restriction of vaccinia virus E3L-specific deletion mutants. Virus Genes. 12(1), 89–94.

Bevilacqua, P.C., Cech, T.R., 1996. Minor-groove recognition of double-stranded RNA by the double-stranded RNA-binding domain from the RNA-activated protein kinase PKR. Biochemistry. 35(31), 9983–9994.

Biron, C.A., Sen, G.C., 2007. Innate Responses to Viral Infections. Fields Virology. 1, 249–278.

Blasco, R., Moss, B., 1991. Extracellular vaccinia virus formation and cell-to-cell virus transmission are prevented by deletion of the gene encoding the 37,000-Dalton outer envelope protein. J. Virol. 65(11), 5910–5920.

Brandt, T., Heck, M.C., Vijaysri, S., Jentarra, G.M., Cameron, J.M., Jacobs, B.L., 2005. The N-terminal domain of the vaccinia virus E3L-protein is required for neurovirulence, but not induction of a protective immune response. Virology. 333(2), 263–270.

Brandt, T.A., Jacobs, B.L., 2001. Both carboxy- and amino-terminal domains of the vaccinia virus interferon resistance gene, E3L, are required for pathogenesis in a mouse model. J. Virol. 75(2), 850–856.

Brewis, I.A., Brennan, P., 2010. Proteomics technologies for the global identification and quantification of proteins. Adv Protein Chem Struct Biol. 80, 1–44.

Broyles, S.S., 2003. Vaccinia virus transcription. J. Gen. Virol. 84(Pt 9), 2293–2303.

Broyles, S.S., Fesler, B.S., 1990. Vaccinia virus gene encoding a component of the

viral early transcription factor. J. Virol. 64(4), 1523–1529.
Carter, G.C., 2005. Entry of the vaccinia virus intracellular mature virion and its interactions with glycosaminoglycans. J. Gen. Virol. 86(5), 1279–1290.
Castelli, J., Wood, K.A., Youle, R.J., 1998. The 2-5A system in viral infection and apoptosis. Biomed. Pharmacother. 52(9), 386–390.
Chakrabarti, A., Jha, B.K., Silverman, R.H., 2011. New insights into the role of RNase L in innate immunity. Journal of Interferon & Cytokine Research. 31(1), 49–57.
Challberg, M.D., Englund, P.T., 1979. Purification and properties of the deoxyribonucleic acid polymerase induced by vaccinia virus. J. Biol. Chem. 254(16), 7812–7819.
Chang, H.W., Watson, J.C., Jacobs, B.L., 1992. The E3L gene of vaccinia virus encodes an inhibitor of the interferon-induced, double-stranded RNA-dependent protein kinase. Proc. Natl. Acad. Sci. U.S.A. 89(11), 4825–4829.
Chang, H.W., Jacobs, B.L., 1993. Identification of a conserved motif that is necessary for binding of the vaccinia virus E3L gene products to double-stranded RNA. Virology. 194(2), 537–547.
Cohen-Chalamish, S., Hasson, A., Weinberg, D., Namer, L.S., Banai, Y., Osman, F., Kaempfer, R., 2009. Dynamic refolding of IFN-γ mRNA enables it to function as PKR activator and translation template. Nature Chemical Biology. Nature Publishing Group, 1–8.
Colamonici, O.R., Domanski, P., Sweitzer, S.M., Larner, A., Buller, R.M., 1995. Vaccinia virus B18R gene encodes a type I interferon-binding protein that blocks interferon alpha transmembrane signaling. J. Biol. Chem. 270(27), 15974–15978.
Cole, J.L., 2007. Activation of PKR: an open and shut case? Trends in Biochemical Sciences. 32(2), 57–62.
Condit, R.C., Moussatché, N., Traktman, P., 2006. In a nutshell: structure and assembly of the vaccinia virion. Adv. Virus Res. 66, 31–124.
Control, C.F.D., 2003. Update: Multistate Outbreak of Monkeypox -- Illinois, Indiana, Kansas, Missouri, Ohio, and Wisconsin, 2003. CDC.
Creagh, E.M., O'Neill, L.A.J., 2006. TLRs, NLRs and RLRs: a trinity of pathogen sensors that co-operate in innate immunity. Trends in Immunology. 27(8), 352–357.
da Fonseca, F.G., Silva, R.L., Marques, J.T., Ferreira, P.C., Kroon, E.G., 1999. The genome of cowpox virus contains a gene related to those encoding the epidermal growth factor, transforming growth factor alpha and vaccinia growth factor. Virus Genes. 18(2), 151–160.
Damaso, C.R., Esposito, J.J., Condit, R.C., Moussatché, N., 2000. An emergent poxvirus from humans and cattle in Rio de Janeiro State: Cantagalo virus may derive from Brazilian smallpox vaccine. Virology. 277(2), 439–449.
Damle, A., Gaikwad, A., Patwardhan, N., Duthade, M., Sheikh, N., Deshmukh, D., 2011. Outbreak of human buffalopox infection. J Glob. Infect. Dis. 3(2): 187-188.

Damon, I.K., 2007. Poxviruses. Fields Virology. 2, 2947–2976.
Davis, J.A., Takagi, Y., Kornberg, R.D., Asturias, F.A., 2002. Structure of the yeast RNA polymerase II holoenzyme: Mediator conformation and polymerase interaction. Mol. Cell. 10(2), 409–415.
Davison, A.J., Moss, B., 1989. Structure of vaccinia virus late promoters. Journal of Molecular Biology. 210(4), 771–784.
Delgado, M., Singh, S., De Haro, S., Master, S., Ponpuak, M., Dinkins, C., Ornatowski, W., Vergne, I., Deretic, V., 2009. Autophagy and pattern recognition receptors in innate immunity. Immunol. Rev. 227(1), 189–202.
Deng, L., Dai, P., Ding, W., Granstein, R.D., Shuman, S., 2006. Vaccinia virus infection attenuates innate immune responses and antigen presentation by epidermal dendritic cells. J. Virol. 80(20), 9977–9987.
Díaz-Guerra, M., Rivas, C., Esteban, M., 1997. Activation of the IFN-inducible enzyme RNase L causes apoptosis of animal cells. Virology. 236(2), 354–363.
Doceul, V., Hollinshead, M., van der Linden, L., Smith, G.L., 2010. Repulsion of superinfecting virions: a mechanism for rapid virus spread. Science. 327(5967), 873–876.
Domingo-Gil, E., Pérez-Jiménez, E., Ventoso, I., Nájera, J.L., Esteban, M., 2008. Expression of the E3L gene of vaccinia virus in transgenic mice decreases host resistance to vaccinia virus and Leishmania major infections. J. Virol. 82(1), 254–267.
Domingo-Gil, E., González, J.M., Esteban, M., 2010. Identification of cellular genes induced in human cells after activation of the OAS/RNaseL pathway by vaccinia virus recombinants expressing these antiviral enzymes. Journal of Interferon & Cytokine Research. 30(3), 171–188.
Donelan, N.R., Basler, C.F., García-Sastre, A., 2003. A recombinant influenza A virus expressing an RNA-binding-defective NS1 protein induces high levels of beta interferon and is attenuated in mice. J. Virol. 77(24), 13257–13266.
Drummond AJ, Ashton B, Buxton S, Cheung M, Cooper A, Duran C, Field M, Heled J, Kearse M, Markowitz S, Moir R, Stones-Havas S, Sturrock S, Thierer T, Wilson A (2011) Geneious v5.4, Available from http://www.geneious.com/
Earl, P.L., Jones, E.V., Moss, B., 1986. Homology between DNA polymerases of poxviruses, herpesviruses, and adenoviruses: nucleotide sequence of the vaccinia virus DNA polymerase gene. Proc. Natl. Acad. Sci. U.S.A. 83(11), 3659–3663.
Essbauer, S., Pfeffer, M., Meyer, H., 2010. Zoonotic poxviruses. Vet. Microbiol. 140(3-4), 229–236.
Evans, E., Klemperer, N., Ghosh, R., Traktman, P., 1995. The vaccinia virus D5 protein, which is required for DNA replication, is a nucleic acid-independent nucleoside triphosphatase. J. Virol. 69(9), 5353–5361.
Evans, E., Traktman, P., 1987. Molecular genetic analysis of a vaccinia virus gene with an essential role in DNA replication. J. Virol. 61(10), 3152–3162.
Garcia, M.A., Gil, J., Ventoso, I., Guerra, S., Domingo, E., Rivas, C., Esteban, M., 2006. Impact of protein kinase PKR in cell biology: from antiviral to

antiproliferative action. Microbiol. Mol. Biol. Rev. 70(4), 1032–1060.
George, C.X., Li, Z., Okonski, K.M., Toth, A.M., Wang, Y., Samuel, C.E., 2009. Tipping the balance: antagonism of PKR kinase and ADAR1 deaminase functions by virus gene products. Journal of Interferon & Cytokine Research. 29(9), 477–487.
Gershon, P.D., Moss, B., 1990. Early transcription factor subunits are encoded by vaccinia virus late genes. Proc. Natl. Acad. Sci. U.S.A. 87(11), 4401–4405.
Gilfoy, F.D., Mason, P.W., 2007. West Nile virus-induced interferon production is mediated by the double-stranded RNA-dependent protein kinase PKR. J. Virol. 81(20), 11148–11158.
Goebel, S.J., Johnson, G.P., Paoletti, E., Perkus, M.E., Davis, S.W., Winslow, J.P., 1990. The complete DNA sequence of vaccinia virus. Virology. 179(1), 247–266.
Gubser, C., Hué, S., Kellam, P., Smith, G.L., 2004. Poxvirus genomes: a phylogenetic analysis. J. Gen. Virol. 85(Pt 1), 105–117.
Guerra, S., Cáceres, A., Knobeloch, K.-P., Horak, I., Esteban, M., 2008. Vaccinia virus E3 protein prevents the antiviral action of ISG15. PLoS Pathogens. 4(7), e1000096.
Ha, S.C., Lokanath, N.K., Van Quyen, D., Wu, C.A., Lowenhaupt, K., Rich, A., Kim, Y.-G., Kim, K.K., 2004. A poxvirus protein forms a complex with left-handed Z-DNA: crystal structure of a Yatapoxvirus Zalpha bound to DNA. Proc. Natl. Acad. Sci. U.S.A. 101(40), 14367–14372.
HAGA, I.R., Bowie, A.G., 2005. Evasion of innate immunity by vaccinia virus. Parasitology. 130 Suppl, S11–25.
Hale, B.G., Steel, J., Medina, R.A., Manicassamy, B., Ye, J., Hickman, D., Hai, R., Schmolke, M., Lowen, A.C., Perez, D.R., García-Sastre, A., 2010. Inefficient control of host gene expression by the 2009 pandemic H1N1 influenza A virus NS1 protein. J. Virol. 84(14), 6909–6922.
Heinicke, L.A., Wong, C.J., Lary, J., Nallagatla, S.R., Diegelman-Parente, A., Zheng, X., Cole, J.L., Bevilacqua, P.C., 2009. RNA Dimerization Promotes PKR Dimerization and Activation☆. Journal of Molecular Biology. 390(2), 319–338.
Heinicke, L.A., Nallagatla, S.R., Hull, C.M., Bevilacqua, P.C., 2011. RNA helical imperfections regulate activation of the protein kinase PKR: Effects of bulge position, size, and geometry. RNA. 17(5), 957–966.
Henderson, D.A., Inglesby, T.V., Bartlett, J.G., Ascher, M.S., Eitzen, E., Jahrling, P.B., Hauer, J., Layton, M., McDade, J., Osterholm, M.T., O'Toole, T., Parker, G., Perl, T., Russell, P.K., Tonat, K., 1999. Smallpox as a biological weapon: medical and public health management. Working Group on Civilian Biodefense., in:, JAMA. pp. 2127–2137.
Ho, C.K., Shuman, S., 1996a. Physical and functional characterization of the double-stranded RNA binding protein encoded by the vaccinia virus E3 gene. Virology. 217(1), 272–284.
Ho, C.K., Shuman, S., 1996b. Mutational analysis of the vaccinia virus E3 protein defines amino acid residues involved in E3 binding to double-stranded RNA. J.

Virol. 70(4), 2611–2614.
Hornung, V., Ellegast, J., Kim, S., Brzózka, K., Jung, A., Kato, H., Poeck, H., Akira, S., Conzelmann, K.-K., Schlee, M., Endres, S., Hartmann, G., 2006. 5'-Triphosphate RNA is the ligand for RIG-I. Science. 314(5801), 994–997.
Hsu, L.-C., Park, J.M., Zhang, K., Luo, J.-L., Maeda, S., Kaufman, R.J., Eckmann, L., Guiney, D.G., Karin, M., 2004. The protein kinase PKR is required for macrophage apoptosis after activation of Toll-like receptor 4. Nature. 428(6980), 341–345.
Hughes, C.M., Blythe, D., Li, Y., Reddy, R., Jordan, C., Edwards, C., Adams, C., Conners, H., Rasa, C., Wilby, S., Russell, J., Russo, K.S., Somsel, P., Wiedbrauk, D.L., Dougherty, C., Allen, C., Frace, M., Emerson, G., Olson, V.A., Smith, S.K., Braden, Z., Abel, J., Davidson, W., Reynolds, M., Damon, I.K., 2011. Vaccinia Virus Infections in Martial Arts Gym, Maryland, USA, 2008. Emerg. Infect. Dis. 17(4), 730–733.
Ichihashi, Y., Oie, M., 1996. Neutralizing epitope on penetration protein of vaccinia virus. Virology. 220(2), 491–494.
Jacobs, B.L., Langland, J.O., 1996. When two strands are better than one: the mediators and modulators of the cellular responses to double-stranded RNA. Virology. 219(2), 339–349.
Jacquemont, B., Roizman, B., 1975. RNA synthesis in cells infected with herpes simplex virus. X. Properties of viral symmetric transcripts and of double-stranded RNA prepared from them. J. Virol. 15(4), 707–713.
Jagus, R., Gray, M.M., 1994. Proteins that interact with PKR. Biochimie. 76(8), 779–791.
Janeway, C.A., 1989. Approaching the asymptote? Evolution and revolution in immunology. Cold Spring Harb. Symp. Quant. Biol. 54 Pt 1, 1–13.
Kahmann, J.D., Wecking, D.A., Putter, V., Lowenhaupt, K., Kim, Y.-G., Schmieder, P., Oschkinat, H., Rich, A., Schade, M., 2004. The solution structure of the N-terminal domain of E3L shows a tyrosine conformation that may explain its reduced affinity to Z-DNA in vitro. Proc. Natl. Acad. Sci. U.S.A. 101(9), 2712–2717.
Katsafanas, G.C., Moss, B., 2004. Vaccinia virus intermediate stage transcription is complemented by Ras-GTPase-activating protein SH3 domain-binding protein (G3BP) and cytoplasmic activation/proliferation-associated protein (p137) individually or as a heterodimer. J. Biol. Chem. 279(50), 52210–52217.
Katze, M.G., DeCorato, D., Safer, B., Galabru, J., Hovanessian, A.G., 1987. Adenovirus VAI RNA complexes with the 68 000 Mr protein kinase to regulate its autophosphorylation and activity. EMBO J. 6(3), 689–697.
Kawai, T., Takahashi, K., Sato, S., Coban, C., Kumar, H., Kato, H., Ishii, K.J., Takeuchi, O., Akira, S., 2005. IPS-1, an adaptor triggering RIG-I- and Mda5-mediated type I interferon induction. Nat. Immunol. 6(10), 981–988.
Kennedy, R.B., Ovsyannikova, I.G., Jacobson, R.M., Poland, G.A., 2009. The immunology of smallpox vaccines. Curr. Opin. Immunol. 21(3), 314–320.
Kim, Y.-G., Muralinath, M., Brandt, T., Pearcy, M., Hauns, K., Lowenhaupt, K.,

Jacobs, B.L., Rich, A., 2003. A role for Z-DNA binding in vaccinia virus pathogenesis. Proc. Natl. Acad. Sci. U.S.A. 100(12), 6974–6979.
Kirkegaard, K., Taylor, M.P., Jackson, W.T., 2004. Cellular autophagy: surrender, avoidance and subversion by microorganisms. Nat. Rev. Microbiol. 2(4), 301–314.
Knutson, B.A., Liu, X., Oh, J., Broyles, S.S., 2006. Vaccinia virus intermediate and late promoter elements are targeted by the TATA-binding protein. J. Virol. 80(14), 6784–6793.
Kwon, J.-A., Rich, A., 2005. Biological function of the vaccinia virus Z-DNA-binding protein E3L: gene transactivation and antiapoptotic activity in HeLa cells. Proc. Natl. Acad. Sci. U.S.A. 102(36), 12759–12764.
Lamkanfi, M., Dixit, V.M., 2009. Inflammasomes: guardians of cytosolic sanctity. Immunol. Rev. 227(1), 95–105.
Langland, J.O., Kash, J.C., Carter, V., Thomas, M.J., Katze, M.G., Jacobs, B.L., 2006. Suppression of proinflammatory signal transduction and gene expression by the dual nucleic acid binding domains of the vaccinia virus E3L proteins. J. Virol. 80(20), 10083–10095.
Langland, J.O., Jacobs, B.L., 1992. Cytosolic double-stranded RNA-dependent protein kinase is likely a dimer of partially phosphorylated Mr = 66,000 subunits. J. Biol. Chem. 267(15), 10729–10736.
Langland, J.O., Jacobs, B.L., 2004. Inhibition of PKR by vaccinia virus: role of the N- and C-terminal domains of E3L. Virology. 324(2), 419–429.
Lecat, A., Piette, J., Legrand-Poels, S., 2010. The protein Nod2: an innate receptor more complex than previously assumed. Biochem. Pharmacol. 80(12), 2021–2031.
Lee, M.S., Kim, Y.-J., 2007. Pattern-recognition receptor signaling initiated from extracellular, membrane, and cytoplasmic space. Mol. Cells. 23(1), 1–10.
Lemaire, P.A., Lary, J., Cole, J.L., 2005. Mechanism of PKR activation: dimerization and kinase activation in the absence of double-stranded RNA. Journal of Molecular Biology. 345(1), 81–90.
Lemaitre, B., Nicolas, E., Michaut, L., Reichhart, J.M., Hoffmann, J.A., 1996. The dorsoventral regulatory gene cassette spätzle/Toll/cactus controls the potent antifungal response in Drosophila adults. Cell. 86(6), 973–983.
Lengyel, P., 1987. Double-stranded RNA and interferon action. J. Interferon Res. 7(5), 511–519.
Lin, S., Chen, W., Broyles, S.S., 1992. The vaccinia virus B1R gene product is a serine/threonine protein kinase. J. Virol. 66(5), 2717–2723.
Liu, L., Zhong, Q., Tian, T., Dubin, K., Athale, S.K., Kupper, T.S., 2010. Epidermal injury and infection during poxvirus immunization is crucial for the generation of highly protective T cell-mediated immunity. Nat. Med. 16(2), 224–227.
Liu, S.-Y., Sanchez, D.J., Cheng, G., 2011. New developments in the induction and antiviral effectors of type I interferon. Curr. Opin. Immunol. 23(1), 57–64.
Ludwig, H., Suezer, Y., Waibler, Z., Kalinke, U., Schnierle, B.S., Sutter, G., 2006. Double-stranded RNA-binding protein E3 controls translation of viral

intermediate RNA, marking an essential step in the life cycle of modified vaccinia virus Ankara. J. Gen. Virol. 87(Pt 5), 1145–1155.
MacNeil, A., Reynolds, M.G., Damon, I.K., 2009. Risks associated with vaccinia virus in the laboratory. Virology. 385(1), 1–4.
Malathi, K., Paranjape, J.M., Bulanova, E., Shim, M., Guenther-Johnson, J.M., Faber, P.W., Eling, T.E., Williams, B.R.G., Silverman, R.H., 2005. A transcriptional signaling pathway in the IFN system mediated by 2"-5-"oligoadenylate activation of RNase L. Proc. Natl. Acad. Sci. U.S.A. 102(41), 14533–14538.
Manche, L., Green, S.R., Schmedt, C., Mathews, M.B., 1992. Interactions between double-stranded RNA regulators and the protein kinase DAI. Mol. Cell. Biol. 12(11), 5238–5248.
Marq, J.-B., Hausmann, S., Luban, J., Kolakofsky, D., Garcin, D., 2009. The double-stranded RNA binding domain of the vaccinia virus E3L protein inhibits both RNA- and DNA-induced activation of interferon beta. J. Biol. Chem. 284(38), 25471–25478.
Marshall, E.E., Geballe, A.P., 2009. Multifaceted evasion of the interferon response by cytomegalovirus. Journal of Interferon & Cytokine Research. 29(9), 609–619.
McFadden, G., 2005. Poxvirus tropism. Nat. Rev. Microbiol. 3(3), 201–213.
McFadden, G., 2010. Killing a killer: what next for smallpox? PLoS Pathogens. 6(1), e1000727.
McFadden, G., Murphy, P.M., 2000. Host-related immunomodulators encoded by poxviruses and herpesviruses. Curr. Opin. Microbiol. 3(4), 371–378.
Medzhitov, R., Preston-Hurlburt, P., Janeway, C.A., 1997. A human homologue of the Drosophila Toll protein signals activation of adaptive immunity. Nature. 388(6640), 394–397.
Melchjorsen, J., Kristiansen, H., Christiansen, R., Rintahaka, J., Matikainen, S., Paludan, S.R., Hartmann, R., 2009. Differential regulation of the OASL and OAS1 genes in response to viral infections. Journal of Interferon & Cytokine Research. 29(4), 199–207.
Meng, X., Jiang, C., Arsenio, J., Dick, K., Cao, J., Xiang, Y., 2009. Vaccinia virus K1L and C7L inhibit antiviral activities induced by type I interferons. J. Virol. 83(20), 10627–10636.
Mercer, J., Helenius, A., 2008. Vaccinia virus uses macropinocytosis and apoptotic mimicry to enter host cells. Science. 320(5875), 531–535.
Mercer, J., Helenius, A., 2010. Apoptotic mimicry: phosphatidylserine-mediated macropinocytosis of vaccinia virus. Ann. N. Y. Acad. Sci. 1209, 49–55.
Meusel, T.R., Kehoe, K.E., Imani, F., 2002. Protein kinase R regulates double-stranded RNA induction of TNF-alpha but not IL-1 beta mRNA in human epithelial cells. J. Immunol. 168(12), 6429–6435.
Meylan, E., Tschopp, J., Karin, M., 2006. Intracellular pattern recognition receptors in the host response. Nature. 442(7098), 39–44.
Meylan, E., Tschopp, J., 2006. Toll-like receptors and RNA helicases: two parallel ways to trigger antiviral responses. Mol. Cell. 22(5), 561–569.

Moss, B., 2006. Poxvirus entry and membrane fusion. Virology. 344(1), 48–54.
Moss, B., 2007. Poxviridae: The Viruses and Their Replication. Fields Virlogy. 2, 2905–2946.
Moussatché, N., Damaso, C.R., McFadden, G., 2008. When good vaccines go wild: Feral Orthopoxvirus in developing countries and beyond. J Infect Dev Ctries. 2(3), 156–173.
Murakami, K.S., Masuda, S., Campbell, E.A., Muzzin, O., Darst, S.A., 2002. Structural basis of transcription initiation: an RNA polymerase holoenzyme-DNA complex. Science. 296(5571), 1285–1290.
Myskiw, C., Arsenio, J., van Bruggen, R., Deschambault, Y., Cao, J., 2009. Vaccinia virus E3 suppresses expression of diverse cytokines through inhibition of the PKR, NF-kappaB, and IRF3 pathways. J. Virol. 83(13), 6757–6768.
Myskiw, C., Arsenio, J., Booy, E.P., Hammett, C., Deschambault, Y., Gibson, S.B., Cao, J., 2011. RNA species generated in vaccinia virus infected cells activate cell type-specific MDA5 or RIG-I dependent interferon gene transcription and PKR dependent apoptosis. Virology. 413(2), 183–193.
Nagasse-Sugahara, T.K., Kisielius, J.J., Ueda-Ito, M., Curti, S.P., Figueiredo, C.A., Cruz, A.S., Silva, M.M.J., Ramos, C.H., Silva, M.C.C., Sakurai, T., Salles-Gomes, L.F., 2004. Human vaccinia-like virus outbreaks in São Paulo and Goiás States, Brazil: virus detection, isolation and identification. Rev. Inst. Med. Trop. Sao Paulo. 46(6), 315–322.
O'Malley, R.P., Mariano, T.M., Siekierka, J., Mathews, M.B., 1986. A mechanism for the control of protein synthesis by adenovirus VA RNAI. Cell. 44(3), 391–400.
Onomoto, K., Yoneyama, M., Fujita, T., 2007. Regulation of antiviral innate immune responses by RIG-I family of RNA helicases. Curr. Top. Microbiol. Immunol. 316, 193–205.
Patel, D.D., Pickup, D.J., 1989. The second-largest subunit of the poxvirus RNA polymerase is similar to the corresponding subunits of procaryotic and eucaryotic RNA polymerases. J. Virol. 63(3), 1076–1086.
Payne, L.G., 1980. Significance of extracellular enveloped virus in the in vitro and in vivo dissemination of vaccinia. J. Gen. Virol. 50(1), 89–100.
Perdiguero, B., Esteban, M., 2009. The interferon system and vaccinia virus evasion mechanisms. Journal of Interferon & Cytokine Research. 29(9), 581–598.
Platanias, L.C., 2005. Mechanisms of type-I- and type-II-interferon-mediated signalling. Nat. Rev. Immunol. 5(5), 375–386.
Poeck, H., Ruland, J., 2011. From virus to inflammation: Mechanisms of RIG-I-induced IL-1β production. Eur J Cell Biol.
Pogo, B.G., Dales, S., 1969. Two deoxyribonuclease activities within purified vaccinia virus. Proc. Natl. Acad. Sci. U.S.A. 63(3), 820–827.
Poltorak, A., He, X., Smirnova, I., Liu, M.Y., Van Huffel, C., Du, X., Birdwell, D., Alejos, E., Silva, M., Galanos, C., Freudenberg, M., Ricciardi-Castagnoli, P., Layton, B., Beutler, B., 1998. Defective LPS signaling in C3H/HeJ and C57BL/10ScCr mice: mutations in Tlr4 gene. Science. 282(5396), 2085–2088.

Prins, K.C., Delpeut, S., Leung, D.W., Reynard, O., Volchkova, V.A., Reid, S.P., Ramanan, P., Cárdenas, W.B., Amarasinghe, G.K., Volchkov, V.E., Basler, C.F., 2010. Mutations abrogating VP35 interaction with double-stranded RNA render Ebola virus avirulent in guinea pigs. J. Virol. 84(6), 3004–3015.

Puissant, B., Combadière, B., 2006. Keeping the memory of smallpox virus. Cell. Mol. Life Sci. 63(19-20), 2249–2259.

Rebouillat, D., Hovanessian, A.G., 1999. The human 2“,5-”oligoadenylate synthetase family: interferon-induced proteins with unique enzymatic properties. J. Interferon Cytokine Res. 19(4), 295–308.

Rice, A.P., Roberts, W.K., Kerr, I.M., 1984. 2-5A accumulates to high levels in interferon-treated, vaccinia virus-infected cells in the absence of any inhibition of virus replication. J. Virol. 50(1), 220–228.

Rimoin, A.W., Mulembakani, P.M., Johnston, S.C., Lloyd Smith, J.O., Kisalu, N.K., Kinkela, T.L., Blumberg, S., Thomassen, H.A., Pike, B.L., Fair, J.N., Wolfe, N.D., Shongo, R.L., Graham, B.S., Formenty, P., Okitolonda, E., Hensley, L.E., Meyer, H., Wright, L.L., Muyembe, J.-J., 2010. Major increase in human monkeypox incidence 30 years after smallpox vaccination campaigns cease in the Democratic Republic of Congo. Proc. Natl. Acad. Sci. U.S.A. 107(37), 16262–16267.

Rivas, C., Gil, J., Mělková, Z., Esteban, M., Díaz-Guerra, M., 1998. Vaccinia virus E3L protein is an inhibitor of the interferon (i.f.n.)-induced 2-5A synthetase enzyme. Virology. 243(2), 406–414.

Roberts, K.L., Smith, G.L., 2008. Vaccinia virus morphogenesis and dissemination. Trends Microbiol. 16(10), 472–479.

Robertson, H.D., Mathews, M.B., 1996. The regulation of the protein kinase PKR by RNA. Biochimie. 78(11-12), 909–914.

Romano, P.R., Zhang, F., Tan, S.L., Garcia-Barrio, M.T., Katze, M.G., Dever, T.E., Hinnebusch, A.G., 1998. Inhibition of double-stranded RNA-dependent protein kinase PKR by vaccinia virus E3: role of complex formation and the E3 N-terminal domain. Mol. Cell. Biol. 18(12), 7304–7316.

Schneider, R.J., Safer, B., Munemitsu, S.M., Samuel, C.E., Shenk, T., 1985. Adenovirus VAI RNA prevents phosphorylation of the eukaryotic initiation factor 2 alpha subunit subsequent to infection. Proc. Natl. Acad. Sci. U.S.A. 82(13), 4321–4325.

Schramm, B., Locker, J.K., 2005. Cytoplasmic organization of POXvirus DNA replication. Traffic. 6(10), 839–846.

Sen, G.C., Lengyel, P., 1992. The interferon system. A bird's eye view of its biochemistry. J. Biol. Chem. 267(8), 5017–5020.

Senkevich, T.G., Ojeda, S., Townsley, A., Nelson, G.E., Moss, B., 2005. Poxvirus multiprotein entry-fusion complex. Proc. Natl. Acad. Sci. U.S.A. 102(51), 18572–18577.

Sharp, T.V., Moonan, F., Romashko, A., Joshi, B., Barber, G.N., Jagus, R., 1998. The vaccinia virus E3L gene product interacts with both the regulatory and the substrate binding regions of PKR: implications for PKR autoregulation. Virology.

250(2), 302–315.
Shchelkunov, S.N., Resenchuk, S.M., Totmenin, A.V., Blinov, V.M., Marennikova, S.S., Sandakhchiev, L.S., 1993. Comparison of the genetic maps of variola and vaccinia viruses. FEBS Lett. 327(3), 321–324.
Shchelkunov, S.N., Totmenin, A.V., Sandakhchiev, L.S., 1996. Analysis of the nucleotide sequence of 23.8 kbp from the left terminus of the genome of variola major virus strain India-1967. Virus Res. 40(2), 169–183.
Sieczkarski, S.B., Whittaker, G.R., 2005. Viral entry. Curr. Top. Microbiol. Immunol. 285, 1–23.
Silva, A.M., Whitmore, M., Xu, Z., Jiang, Z., Li, X., Williams, B.R.G., 2004. Protein kinase R (PKR) interacts with and activates mitogen-activated protein kinase kinase 6 (MKK6) in response to double-stranded RNA stimulation. J. Biol. Chem. 279(36), 37670–37676.
Simpson-Holley, M., Kedersha, N., Dower, K., Rubins, K.H., Anderson, P., Hensley, L.E., Connor, J.H., 2011. Formation of antiviral cytoplasmic granules during orthopoxvirus infection. J. Virol. 85(4), 1581–1593.
Singh, M., Castillo, D., Patel, C.V., Patel, R.C., 2011. Stress-induced phosphorylation of PACT reduces its interaction with TRBP and leads to PKR activation. Biochemistry.
Smee, D.F., 2008. Progress in the discovery of compounds inhibiting orthopoxviruses in animal models. Antivir. Chem. Chemother. 19(3), 115–124.
Smith, G.L., Vanderplasschen, A., Law, M., 2002. The formation and function of extracellular enveloped vaccinia virus. J. Gen. Virol. 83(Pt 12), 2915–2931.
Smith, G.L., Murphy, B.J., Law, M., 2003. Vaccinia virus motility. Annu. Rev. Microbiol. 57, 323–342.
Smith, G.L., Law, M., 2004. The exit of vaccinia virus from infected cells. Virus Res. 106(2), 189–197.
Talon, J., Horvath, C.M., Polley, R., Basler, C.F., Muster, T., Palese, P., García-Sastre, A., 2000. Activation of interferon regulatory factor 3 is inhibited by the influenza A virus NS1 protein. J. Virol. 74(17), 7989–7996.
Taniguchi, T., Takaoka, A., 2001. A weak signal for strong responses: interferon-alpha/beta revisited. Nat. Rev. Mol. Cell Biol. 2(5), 378–386.
Timms, J.F., Cramer, R., 2008. Difference gel electrophoresis. Proteomics. 8(23-24), 4886–4897.
Tolonen, N., Doglio, L., Schleich, S., Krijnse-Locker, J., 2001. Vaccinia virus DNA replication occurs in endoplasmic reticulum-enclosed cytoplasmic mini-nuclei. Mol. Biol. Cell. 12(7), 2031–2046.
Twardzik, D.R., Brown, J.P., Ranchalis, J.E., Todaro, G.J., Moss, B., 1985. Vaccinia virus-infected cells release a novel polypeptide functionally related to transforming and epidermal growth factors. Proc. Natl. Acad. Sci. U.S.A. 82(16), 5300–5304.
Unterholzner, L., Bowie, A.G., 2008. The interplay between viruses and innate immune signaling: recent insights and therapeutic opportunities. Biochem. Pharmacol. 75(3), 589–602.

Upton, C., Slack, S., Hunter, A.L., Ehlers, A., Roper, R.L., 2003. Poxvirus orthologous clusters: toward defining the minimum essential poxvirus genome. J. Virol. 77(13), 7590–7600.

Valentine, R., Smith, G.L., 2010. Inhibition of the RNA polymerase III-mediated dsDNA-sensing pathway of innate immunity by vaccinia virus protein E3. J. Gen. Virol. 91(Pt 9), 2221–2229.

Van Vliet, K., Mohamed, M.R., Zhang, L., Villa, N.Y., Werden, S.J., Liu, J., McFadden, G., 2009. Poxvirus proteomics and virus-host protein interactions. Microbiol. Mol. Biol. Rev. 73(4), 730–749.

Vanderplasschen, A., Hollinshead, M., Smith, G.L., 1998. Intracellular and extracellular vaccinia virions enter cells by different mechanisms. J. Gen. Virol. 79 (Pt 4), 877–887.

Werden, S.J., Rahman, M.M., McFadden, G., 2008. Poxvirus host range genes. Adv. Virus Res. 71, 135–171.

Willis, K.L., Langland, J.O., Shisler, J.L., 2011. Viral double-stranded RNAs from vaccinia virus early or intermediate gene transcripts possess PKR activating function, resulting in NF-kappaB activation, when the K1 protein is absent or mutated. J. Biol. Chem. 286(10), 7765–7778.

Xiang, Y., Latner, D.R., Niles, E.G., Condit, R.C., 2000. Transcription elongation activity of the vaccinia virus J3 protein in vivo is independent of poly(A) polymerase stimulation. Virology. 269(2), 356–369.

Xiang, Y., Condit, R.C., Vijaysri, S., Jacobs, B., Williams, B.R.G., Silverman, R.H., 2002. Blockade of interferon induction and action by the E3L double-stranded RNA binding proteins of vaccinia virus. J. Virol. 76(10), 5251–5259.

Yoneyama, M., Kikuchi, M., Natsukawa, T., Shinobu, N., Imaizumi, T., Miyagishi, M., Taira, K., Akira, S., Fujita, T., 2004. The RNA helicase RIG-I has an essential function in double-stranded RNA-induced innate antiviral responses. Nat. Immunol. 5(7), 730–737.

Yoneyama, M., Kikuchi, M., Matsumoto, K., Imaizumi, T., Miyagishi, M., Taira, K., Foy, E., Loo, Y.-M., Gale, M., Akira, S., Yonehara, S., Kato, A., Fujita, T., 2005. Shared and unique functions of the DExD/H-box helicases RIG-I, MDA5, and LGP2 in antiviral innate immunity. J. Immunol. 175(5), 2851–2858.

Yu, M., Levine, S.J., 2011. Toll-like receptor 3, RIG-I-like receptors and the NLRP3 inflammasome: Key modulators of innate immune responses to double-stranded RNA viruses. Cytokine Growth Factor Rev.

Yuwen, H., Cox, J.H., Yewdell, J.W., Bennink, J.R., Moss, B., 1993. Nuclear localization of a double-stranded RNA-binding protein encoded by the vaccinia virus E3L gene. Virology. 195(2), 732–744.

Zhang, P., Jacobs, B.L., Samuel, C.E., 2008. Loss of protein kinase PKR expression in human HeLa cells complements the vaccinia virus E3L deletion mutant phenotype by restoration of viral protein synthesis. J. Virol. 82(2), 840–848.

Zhang, Y., Keck, J.G., Moss, B., 1992. Transcription of viral late genes is dependent on expression of the viral intermediate gene G8R in cells infected with an inducible conditional-lethal mutant vaccinia virus. J. Virol. 66(11), 6470–6479.

Zheng, X., Bevilacqua, P.C., 2004. Activation of the protein kinase PKR by short double-stranded RNAs with single-stranded tails. RNA. 10(12), 1934–1945.
Zhou, A., Paranjape, J.M., Hassel, B.A., Nie, H., Shah, S., Galinski, B., Silverman, R.H., 1998. Impact of RNase L overexpression on viral and cellular growth and death. J. Interferon Cytokine Res. 18(11), 953–961.

APPENDIX

APPENDIX 1

Alignment amino acid sequences of E3L orthologs from five *Chordopoxvirinae* members: Vaccinia virus Copenhagen E3L (M35027), Myxoma virus 029L (AF170726), Capripox virus 034L (NC_004002), Yaba Monkey Tumor Virus 034L (AY386371) and Swinepox virus 032L (NC_003389). Vaccinia COP sequence used as reference and consensus sequence displayed. Sequence alignment performed using Geneious v5.4 (Drummond et al., 2011).

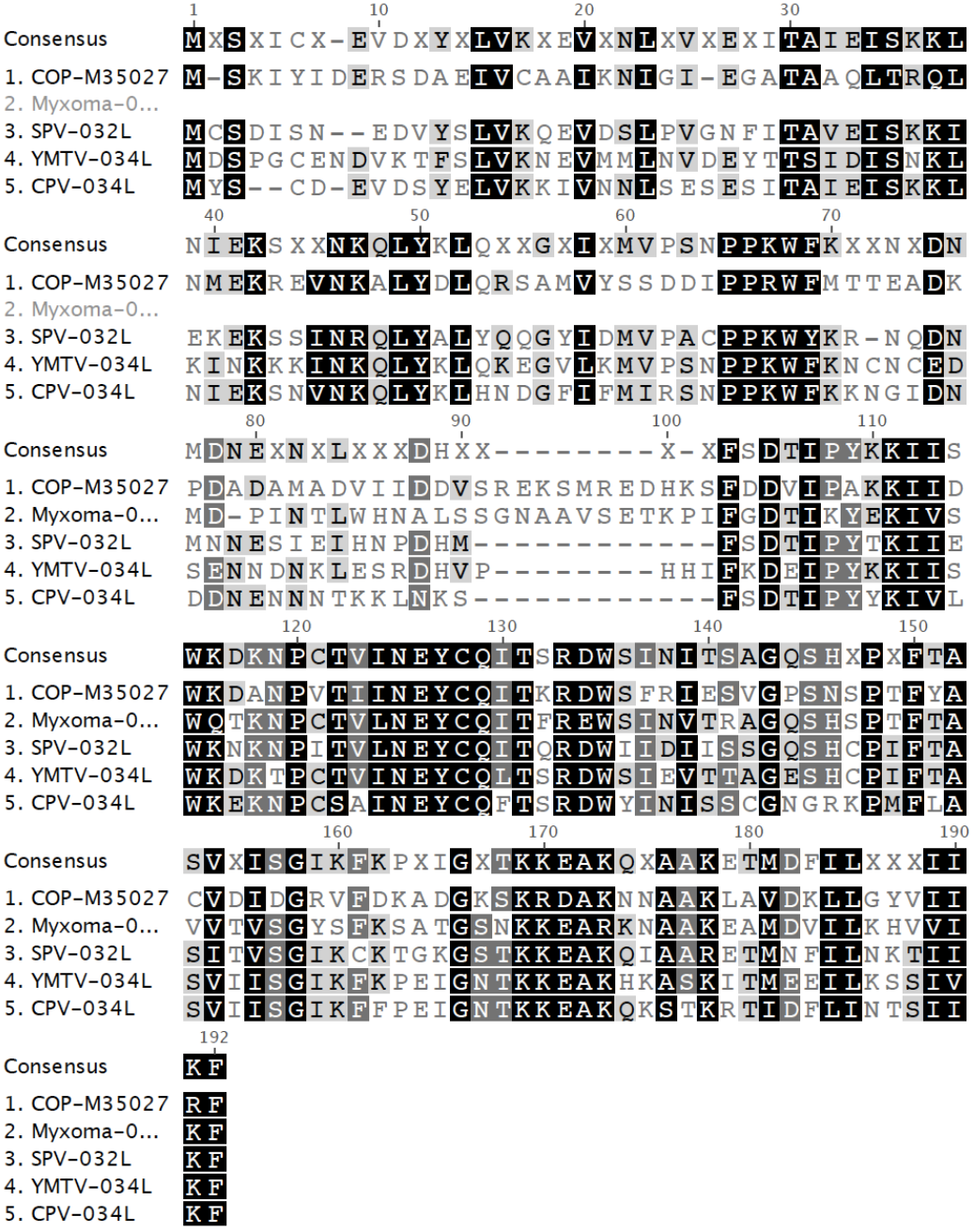

APPENDIX 2A

Poly I:C pulldown in BHK21 cells of mutated highly conserved E3 residues (Table 2). Pre and post-pulldown samples shown. The pJS5 plasmid bearing an individual E3L mutant transfected following 1 hr infection with MOI 0.2 COP-ΔE3L to generate recombinant Vaccinia virus expressing the desired mutant E3. Samples collected following overnight growth. Western blots probed with rabbit polyclonal vvE3L #2 antibody.

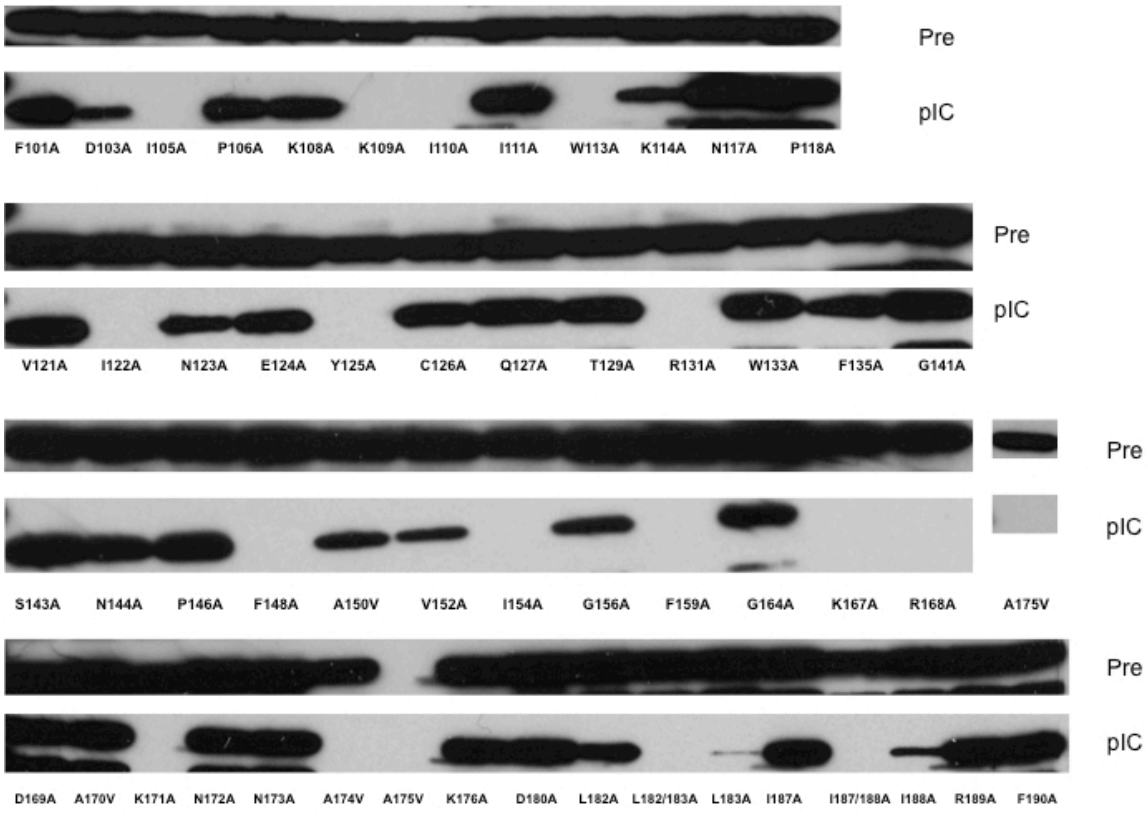

APPENDIX 2B

Poly I:C pulldown in BHK21 cells of mutated low conservation E3 residues (Table 3). Pre and post-pulldown samples shown. The pJS5 plasmid bearing an individual E3L mutant transfected following 1 hr infection with MOI 0.2 COP-ΔE3L to generate recombinant Vaccinia virus expressing the desired mutant E3. Samples collected following overnight growth. Positive binding results for boxed samples presented in separate blots. Western blots probed with rabbit polyclonal vvE3L #1/#2 antibody.

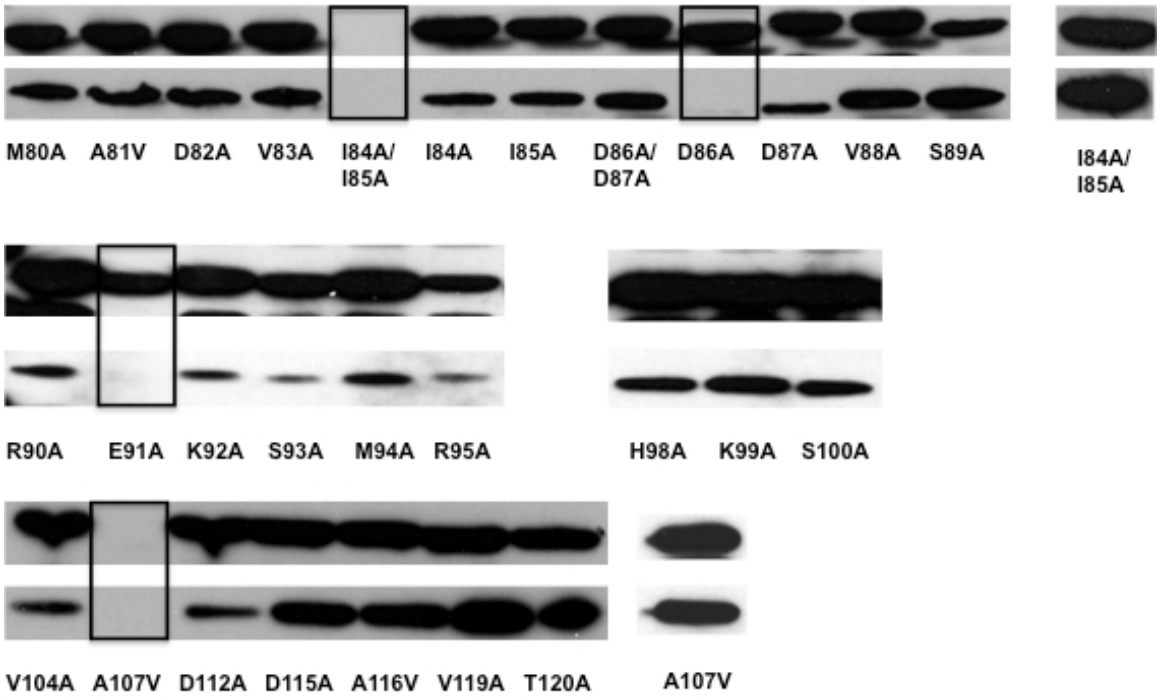

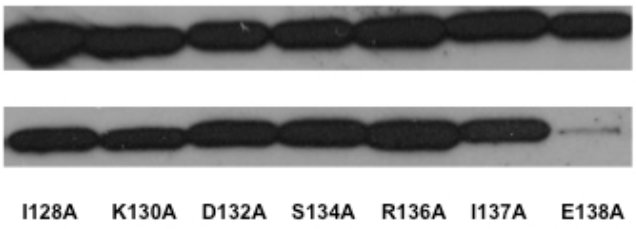

I128A K130A D132A S134A R136A I137A E138A

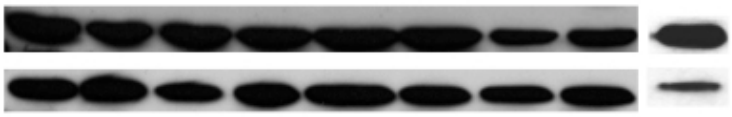

S139A V140A P142A S145A T147A Y149A C151A D153A D155A

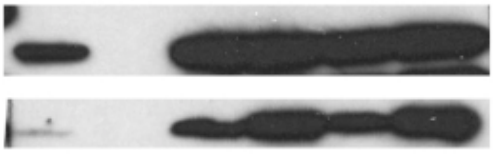

REV ΔE3L R157A V158A D160A K161A

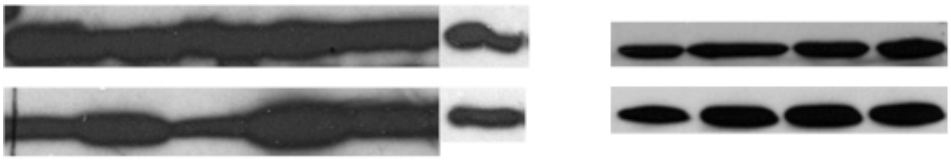

A162V D163A K165A S166A L177A V179A A178V K181A G184A Y185A

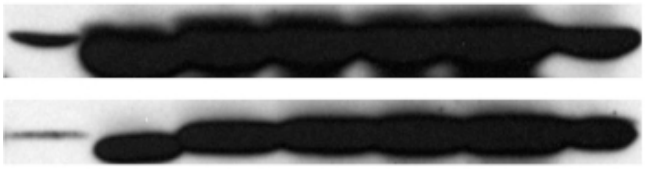

REV D86/ D87A E91A E96A D97A D102A V186A

APPENDIX 3

Pulldown in HeLa cells to confirm differential interaction of mutant E3 constructs with endogenous proteins found by 2D DIGE analysis. A) Verification of Expression and GST-pulldown. B) Verification of 2D DIGE interactions on pulldown lysates. HeLa monolayers grown in 100mm dishes transfected with pJS5 constructs expressing GST-E3L, GST-Δ175, GST- ΔC111 or GST for 2 hrs prior to infection with COP-REV at an MOI of 2. Collected under non-denaturing conditions 10 hpi for pulldown with Glutathione beads. Samples probed for β-Actin, vvE3L #1/2, GST, LANCL1, EEF1G, EEF1A1 and CBR1 antibodies.